



OPEN ACCESS

EDITED BY

Haijun Song,
China University of Geosciences
Wuhan, China

REVIEWED BY

Mohammad Alqudah,
Yarmouk University, Jordan
Arindam Chakraborty,
Universiti Malaya, Malaysia

*CORRESPONDENCE

Amr S. Zaky,
✉ amrsaid86@science.menofia.edu.eg
Luigi Jovane,
✉ jovane@usp.br

RECEIVED 01 June 2024

ACCEPTED 26 July 2024

PUBLISHED 20 August 2024

CITATION

Abu Shama A, El-Nahrawy S, Farouk S,
Jovane L, Al-Kahtany K and Zaky AS (2024)
Calcareous nannofossil biostratigraphy,
bioevents, and palaeoecological
interpretation of the lower-middle Miocene
outcrops in west central Sinai (Egypt).
Front. Earth Sci. 12:1442241.
doi: 10.3389/feart.2024.1442241

COPYRIGHT

© 2024 Abu Shama, El-Nahrawy, Farouk,
Jovane, Al-Kahtany and Zaky. This is an
open-access article distributed under the
terms of the [Creative Commons Attribution
License \(CC BY\)](https://creativecommons.org/licenses/by/4.0/). The use, distribution or
reproduction in other forums is permitted,
provided the original author(s) and the
copyright owner(s) are credited and that the
original publication in this journal is cited, in
accordance with accepted academic practice.
No use, distribution or reproduction is
permitted which does not comply with
these terms.

Calcareous nannofossil biostratigraphy, bioevents, and palaeoecological interpretation of the lower-middle Miocene outcrops in west central Sinai (Egypt)

Aziz Abu Shama¹, Sara El-Nahrawy¹, Sherif Farouk²,
Luigi Jovane^{3*}, Khaled Al-Kahtany⁴ and Amr S. Zaky^{3,5*}

¹Department of Geology, Faculty of Science, Kafrelsheikh University, Kafr El-Sheikh, Egypt,

²Exploration Department, Egyptian Petroleum Research Institute, Nasr City, Egypt, ³Instituto
Oceanográfico da Universidade de São Paulo, Praça do Oceanográfico, São Paulo, Brazil,

⁴Department of Geology and Geophysics, College of Science, King Saud University, Riyadh, Saudi
Arabia, ⁵Geology Department, Faculty of Science, Menoufia University, Shebin El-Kom, Egypt

The Burdigalian/Langhian (B/L) boundary has not yet been designated as a Global Stratotype Section and Point (GSSP), despite various proposed zonal schemes. In the Gulf of Suez region of Egypt, the Burdigalian–Langhian successions are notable for hosting significant hydrocarbon reservoirs within a tectonic rift setting. Therefore, biostatigraphy plays a crucial role in exploration endeavors in this area. The nannofossil biostratigraphy is investigated in two sections, Wadi Baba and Wadi Gharandel, of the lower-middle Miocene from west-central Sinai. Three biozones, NN3 (*Sphenolithus belemnos*) Zone, NN4 (*Helicosphaera ampliaperta*) Zone, and NN5 (*Sphenolithus heteromorphus*) Zone, are identified from the studied interval. The NN4 Zone could be divided into MNN4a/b and MNN4c. Important bioevents are discussed, such as the *S. heteromorphus* paracme interval and the first occurrence and evolution of the *Discoaster exilis* and *Discoaster variabilis* groups. Based on the cluster analysis, the recorded taxa can be subdivided into four groups that reflect their palaeoclimatic preferences. The paleoecological interpretation of the studied Rudies Formation indicates prevailing cool and eutrophic nutrient conditions based on the dominance of taxa such as *Coccolithus pelagicus*, *Reticulofenestra minuta*, and *Cyclicargolithus floridanus*. The nannofossil taxa responses to sea level curve are interpreted. Fluctuations in taxa abundance and diversity indicate a slight rise in the sea level at the base of the Burdigalian followed by sudden drop in the sea level at the middle Burdigalian. High sea-level conditions prevailed again until the B/L boundary. During the Langhian period, many small-scale fluctuations in sea-level curve are detected.

KEYWORDS

calcareous microfossils, Cenozoic, past sea level, Rudies Formation, Burdigalian, Langhian, paleoenvironment, Egypt

1 Introduction

The Miocene epoch (ca. 23.03–5.33 Ma) is one of the most interesting epochs in the geologic record in terms of the global climate changes and sea-level oscillations (Frigola et al., 2018; Khalifa et al., 2024). It has been divided into three sub-epochs; the early Miocene (23.03–15.97 Ma), the middle Miocene (15.97–11.63 Ma), and the late Miocene (11.63–5.33 Ma) (Bradshaw, 2021). Important palaeoclimatic changes and magnetic chronostratigraphic studies have also been conducted on this crucial epoch (Lourens et al., 2004; Turco et al., 2011; Jovane et al., 2019; Jovane et al., 2020). The Miocene Epoch showed generally warm climate that culminated in the Mid-Miocene Climatic Optimum (MMCO) at roughly 17–14 Ma, followed immediately by shift towards global cooling may be linked to the expansion of Antarctic glaciers during the Middle Miocene Climate Transition (MMCT) at about 14.2–13.8 Ma (Shevenell et al., 2004; Shevenell et al., 2008; Jovane et al., 2020). Therefore, sea-levels during the Miocene were typically higher than those today, the emergence of the Antarctic Circumpolar Current (ACC) had a significant impact on atmospheric and marine circulation patterns worldwide due to the separation of Antarctica from Australia (Colleoni et al., 2022).

Many attempts have been made to reveal the global microfossil bio-events that occur across the Burdigalian/Langhian (B/L) boundary (Rio et al., 1990; Raffi and Flores, 1995; Fornaciari et al., 1996; Lourens et al., 2004; Aziz et al., 2008; Di Stefano et al., 2008; Iaccarino et al., 2011; Backman et al., 2012; Raffi et al., 2016; Agnini et al., 2017; El-Naby et al., 2017; Chakraborty et al., 2019; Chakraborty et al., 2021).

This work establishes high-resolution biostratigraphic studies of the B/L boundary in the Miocene outcrops on the eastern margin of the Gulf of Suez (GOS), Egypt. Also, it focuses on the calcareous nannofossil assemblage and significant bioevents at the B/L boundary within the Rudies Formation.

Miocene deposits in the GOS are important due to their hydrocarbon-rich reservoirs (e.g., NSSC (National Stratigraphic Sub-Committee), 1974; El-Heiny and Martini, 1981; Andrawis and Abdel Malik, 1981; El-Heiny and Morsi, 1992; Moustafa, 1993; El-Azabi, 1996, El-Azabi, 1997, El-Azabi, 1004; Abul-Nasr and Salama, 1999; El-Deeb et al., 2004; Mandur, 2009; Boukhary et al., 2012; Hewaidy et al., 2014; Hewaidy et al., 2016; Abd-El Naby and Salama, 1999; El-Naby et al., 2017; Shahin and El Baz, 2021; Ayyad et al., 2020; Ayyad et al., 2022). However, due to the lateral and vertical facies changes caused by the rifting event, defining the age of the Miocene units precisely and achieving biostratigraphic correlation is challenging. The syn-rift deposits of the GOS contain the most important petroleum reservoirs in the province. It includes the clastic and carbonate sequence of the Nukhul, Rudies, Kareem and Belayim formations. The Rudies Formation is the most productive for oil in the GOS and can be subdivided into Lower Burdigalian and Upper Langhian Rudies units (Moustafa and Khalil, 1990). It is also considered a rich potential source rock in the deep basins (Alsharhan, 2003).

Detailed nannofossil biostratigraphic events used globally around the lower/middle Miocene boundary, as well as the use of nannofossils as a tool for clustering and interpreting prevailing paleoecological conditions, were not addressed in previous work on the GOS and its margins. This study will provide a detailed

comparison of the studied sediments with global nannofossil bioevents around the boundary and reconstruct the paleoecological conditions.

The main aims of this study are to: 1) establish a regional biostratigraphic scheme for the Rudies Formation; 2) correlate the present study with significant global nannofossil bioevents across the B/L boundary; 3) interpret the paleoclimatic and paleoenvironmental conditions that prevailed during the deposition of the Rudies Formation, as well as the biotic response to global sea level oscillations.

2 Geologic setting

The GOS gained its fame because it is the principal hydrocarbon-producing prospect in Egypt. The oil is being produced mostly from Miocene sediment reservoirs, both in onshore and offshore fields (El Ayouy, 1990). This province was formed as a result of the divergence between the African and Arabian plates. The rifting started in late Oligocene–Miocene time (Moustafa, 1993; Bosworth and McClay, 2001). In the middle Burdigalian (19–17 Ma), a rapid tectonic subsidence occurred, and sedimentary deposits were formed in fault-impacted basins (Patton et al., 1994). This tectonic subsidence is called a mid-clysmic event, 17 Ma (Garfunkel and Batrov, 1977).

Lithostratigraphically, the GOS is classified into Paleozoic to lower Eocene pre-rift, Miocene syn-rift, and Quaternary post-rift successions (Plaziat et al., 1998). The syn-rift Miocene clastic/carbonate (Rudeis, Kareem, and Belayim formations) are well demonstrated in the eastern margin blocks of the GOS. The Rudeis Formation is overlain by the Kareem Formation and underlain by the Nukhul Formation. They show variation in lateral facies and thickness associated with the tectonic activity and subsidence that prevailed during their deposition (Sellwood and Netherwood, 1984). The Kareem and Rudeis formations are probable oil-prone source rocks; the Belayim Formation is categorized as an oil- and gas-prone source rock (El Ayouy, 1990). The Rudeis Formation comprises siliciclastic interbedded with limestones (Bosworth et al., 1998), which are synonymous to the *Globigerina* marl reported by Hume et al. (1920) in the northern part of the province. The Rudies Formation was deposited within extensive accommodation spaces at the downward movements of the dominant listric and normal faults controlling the basin, allowing the deposition of deep marine deposits (Moustafa and Khalil, 1990).

3 Lithostratigraphy

The studied Rudies Formation was presented by Ghorab et al. (1964) to describe the rocks of Rudies-2 well (west-central Sinai) from depth 1840–2620 m. The Rudies Formation is subdivided into three members as follows: Mheiherrat/Hawara, Asl, and Mreir (NSSC, 1974). For this study, a detailed litho- and biostratigraphic study of the Rudies Formation from two sections, Wadi Baba and Wadi Gharandel, was carried out (Figure 1). The Mheiherrat/Hawara Member unconformably overlies the Nukhul Formation at the Wadi Baba section and forms the basal part of the Wadi Gharandel section. It is composed of alternations of marl and sandy marl with thin

layers of sandstone and burrowed sandy limestone (Figures 2, 3). It consists of shales intercalated with limestone at the upper part of the Wadi Gharandel section (Hawara Member) (Figure 3). It compasses a thickness of about 57.5 m at Wadi Baba and 42.5 m at Wadi Gharandel. The Asl Member is composed of forming walls of sandy limestone and marl with laminations of sandstone and sandy marl (Figure 4A). It ended with thin layers of sandy limestone with chert and gravel and laminated sandstone. It reaches a thickness of about 10 m in Wadi Gharandel and 37.5 m at Wadi Baba. At Wadi Baba, the Mreir Member is composed of marl at the lower part and sandy limestone, argillaceous limestone, and shales at the upper part (26 m). It is composed of sandy marl with intercalations of mudstone at the lower part overlying sandy marl and sandy limestone at Wadi Gharandel (60 m) (Figures 3, 4B).

4 Materials and methods

A total of 187 samples were examined for calcareous nannofossil biostratigraphy from Wadi Baba (28° 57'271" N, 33°15'784"E) and Wadi Gharandel (29° 14'67"N, 33°01'891"E) sections at west-central Sinai, Egypt (Figure 1). Calcareous nannofossil biostratigraphy was based on 86 samples at Wadi Baba and 101 samples at Wadi Gharandel. Sample interval varied from 20 cm to 4 m. Smear slides for the nannofossil study were prepared using the methods of Perch-Nielsen (1985) and Bown and Young (1998) and examined using transmitted-light (TL) in cross-polarised (XPL) and phase-contrast (pH) modes of an Olympus TH4-200 microscope under $\times 1,000$ magnification. For datum levels, we used FO (first occurrence), LO (last occurrence), PB (paracme beginning), PE (paracme end) and LCO (last common occurrence). The zonal schemes that were employed in nannofossil biostratigraphic investigations are Okada and Bukry (1980), Martini (1971), Di Stefano et al. (2008) for the subdivision of the Zone NN4, Bergen et al. (2019) and Backman et al. (2012). The qualitative and quantitative nannofossil taxa are counted from 100 to 600 individuals except for a few samples that show low abundance and scarcity. The species were grouped into clusters and diversity parameters such as dominance index, Shannon-Weiner diversity index and species richness were described using PAST4 software (Hammer et al., 2001; Hammer and Harper, 2006).

5 Results

For the present study, a detailed litho-biostratigraphic analysis of the Rudies Formation from two sections, Wadi Baba and Wadi Gharandel, were carried out. The detailed calcareous nannofossil biostratigraphy, bioevents, assemblages, and diversity will be presented as follows:

5.1 Calcareous nannofossil biostratigraphy and bioevents

Based on the first occurrence (FO) and the last occurrence (LO) of the nannofossil marker species, three biozones were identified (Figure 5). Important marker species are depicted and labeled on

Figure 6. The preservation of nannofossil in the studied samples is varied with the age of sediments and the assemblage. The preservation of the most abundant *Coccolithus* is very well in relative to the nannofossil assemblage. *Reticulofenestra* group in which *Reticulofenestra haqii* and *Reticulofenestra minuta* are the most abundant shows moderate to good preservation, but sometimes it shows a partial dissolution in their outer rims or the central areas. Although the *Discoaster* preservation varies even in the same sample, the definition of the Burdigalian/Langhian boundary in this work is depending on the well preserved marker *discoaster* species. The *Discoaster deflandrei* is the most dominant from of this taxon in the Lower Miocene sediments and well preserved with no dissolution but sometimes it shows partial dissolution within the Middle Miocene. *Discoaster druggii* show the same trend of *D. deflandrei*. At the base of the Middle Miocene, the new evolved *Discoasters* show different preservation in the same sample. These features of preservation may be related to the diagenetic processes such as calcite overgrown and/or chemical dissolution. Therefore, this study cannot use the analysis of preservation state and nannofossil dissolution of individual nannofossil taxa as proxy for CCD variation and to constrain the history of CCD fluctuations (e.g., Pea et al., 2011).

The *S. belemnus* Zone (NN3) of Bramlette and Wilcoxon (1967), emended by Martini (1971), is recorded from the basal parts of the studied sections (Figures 2, 3). It is identified from the LO of *Triquetrohabdulus carinatus* to the LO of *Sphenolithus belemnus*. It is correlated with the CN2 *S. belemnus* Zone of Okada and Bukry (1980) and is compatible with the CNM5 Zone (Figure 5) of Backman et al. (2012). It spans 30 m at Wadi Baba (samples 71–95) and 7.5 m at Wadi Gharandel (samples G1 to G9) and is representative of important species. The LO *S. belemnus* (17.96 Ma) (e.g., Fornaciari et al., 1993; Fornaciari and Rio, 1996; McGonigal, 2004) defines the boundary between NN3 and NN4 in the Martini (1971) zonation. The most distinct species in this zone are *Sphenolithus disbelemnus*, *S. belemnus*, *Sphenolithus compactus*, *Discoaster druggii*, *Helicosphaera mediterranea*, and *Helicosphaera euphratis*.

The *H. ampliaptera* Zone (NN4) of Bramlette and Wilcoxon (1967), emended by Martini (1971), marks the time from the LO of *S. belemnus* to the LO of *H. ampliaptera*. It may be equivalent to the CNM6/lower part of the CNM7 zones of Backman et al. (2012). The CNM 6 Zone is defined from the FO of *Sphenolithus heteromorphus* to the FO of *Discoaster signus*. It distinguished by the common occurrence of *Helicosphaera ampliaptera* as well as the presence of *D. deflandrei* group. The lower interval of CNM 6 Zone is well defined. Backman et al. (2012) marked the base of CNM 7 Zone by the FO of *D. signus*, but the species is not recorded in the studied sections. The *Discoaster petaliformis* with approximately similar age (15.7 Ma) is recorded and is used to define the base of CNM 7.

The FO of *S. heteromorphus* at 17.75 Ma is observed in the lower part of Zone NN4 and used as a primary nannofossil event to approximate the base of NN4 (Fornaciari and Rio, 1996; Lourens et al., 2004; Raffi et al., 2006). The FO of the species is observed at 17.79 Ma and its common occurrence at 17.39 Ma (Bergen et al., 2019). The FO of *S. heteromorphus* occurs in sample 96 at Wadi Baba and sample G11 at Wadi Gharandel. The LO of *H. ampliaptera* is recorded in sample G75 at the Wadi Gharandel

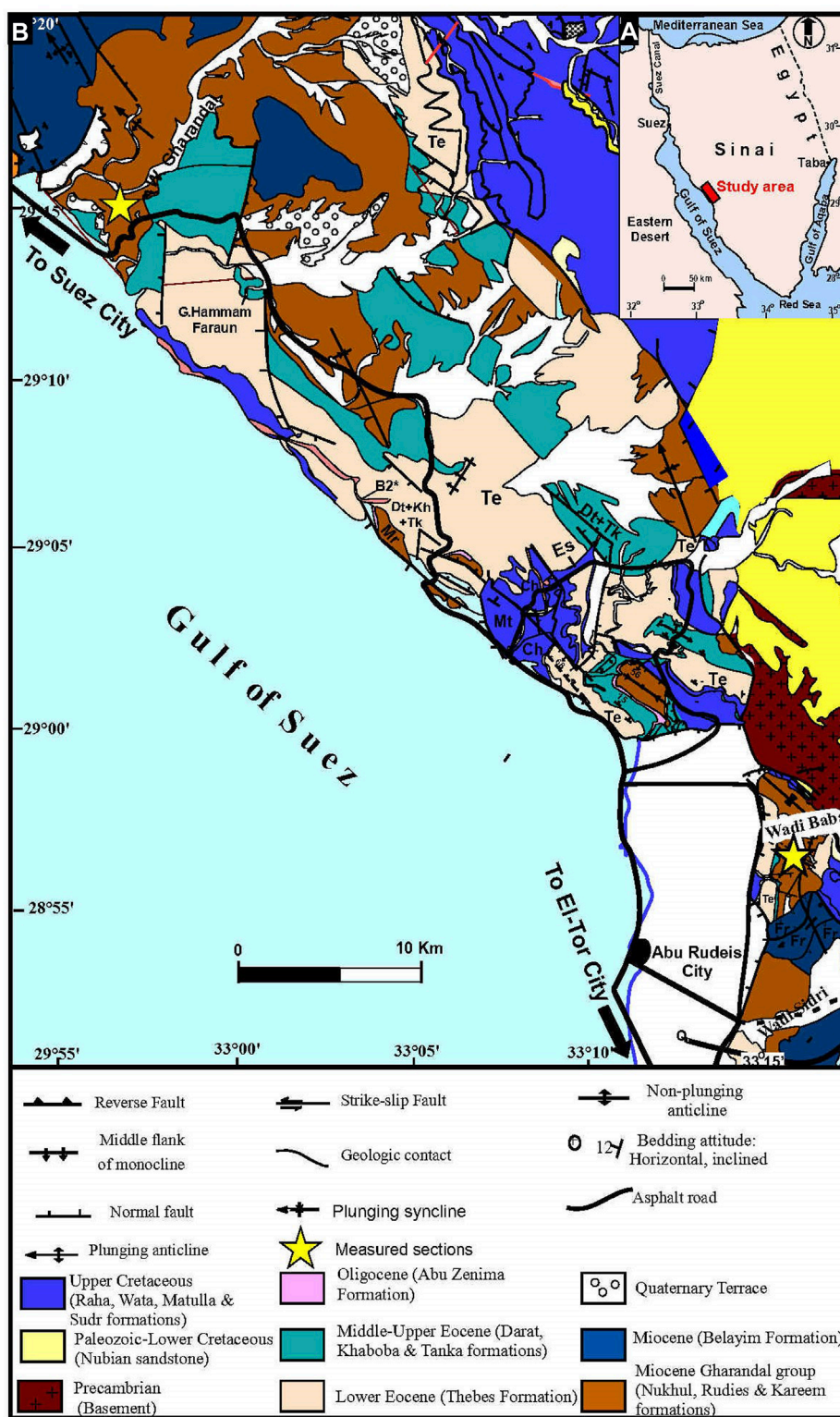
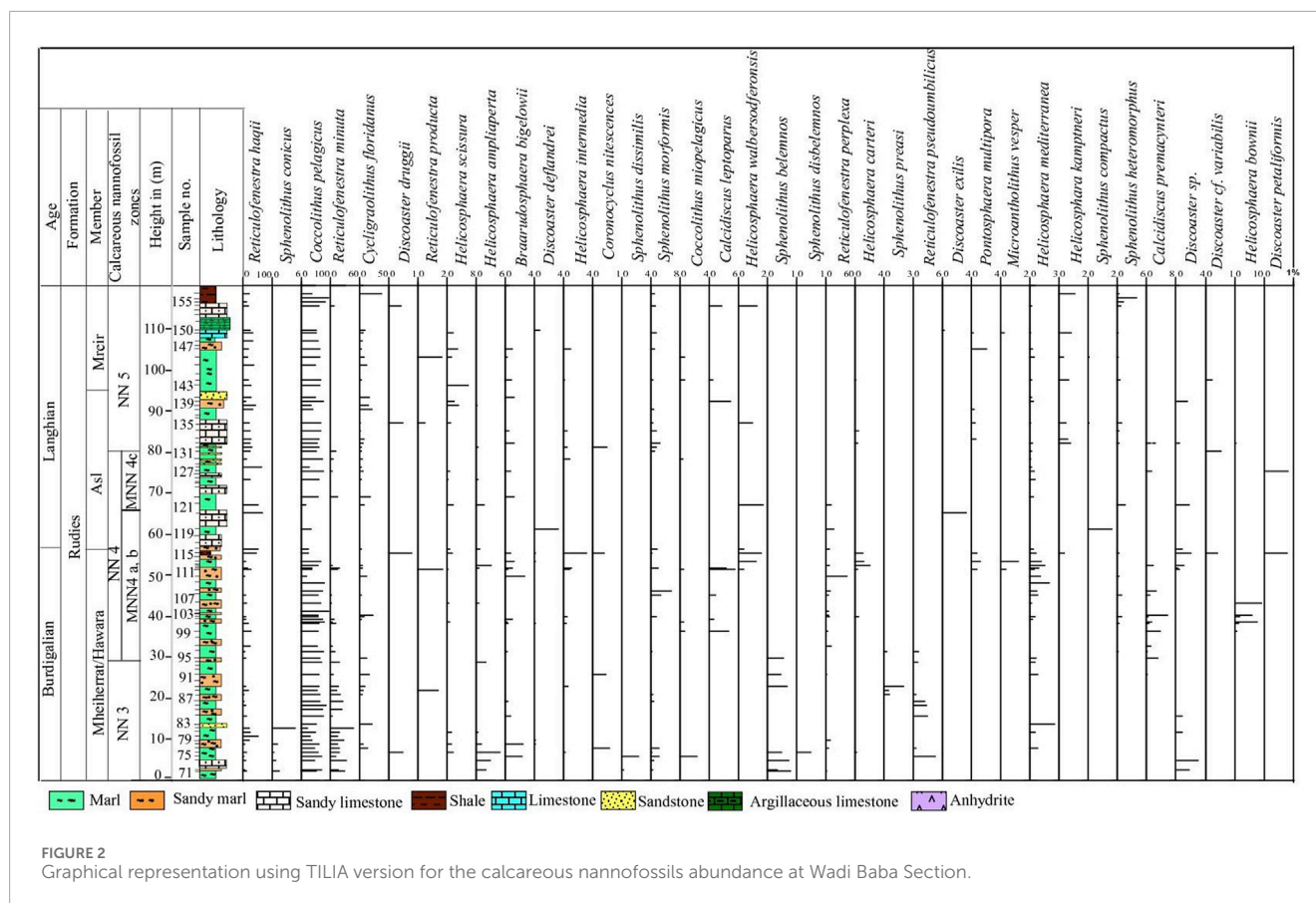


FIGURE 1 (A) Location of the study area, Egypt; (B) Geological map of the study area in west-central Sinai, Egypt (modified after Moustafa, 2004).

section and in sample 139 at the Wadi Baba section. The LO of *H. ampliaptera* is noticed at 14.89 Ma (Bergen et al., 2019). The thickness of this zone is about 50 m at Wadi Baba and 65 m at

Wadi Gharandel. The FO of *calcidiscus premacintyre* is observed in the lower part of Zone NN4 (Maiorano and Monechi, 1998), but other authors have used the FO of *C. premacintyre* as a primary

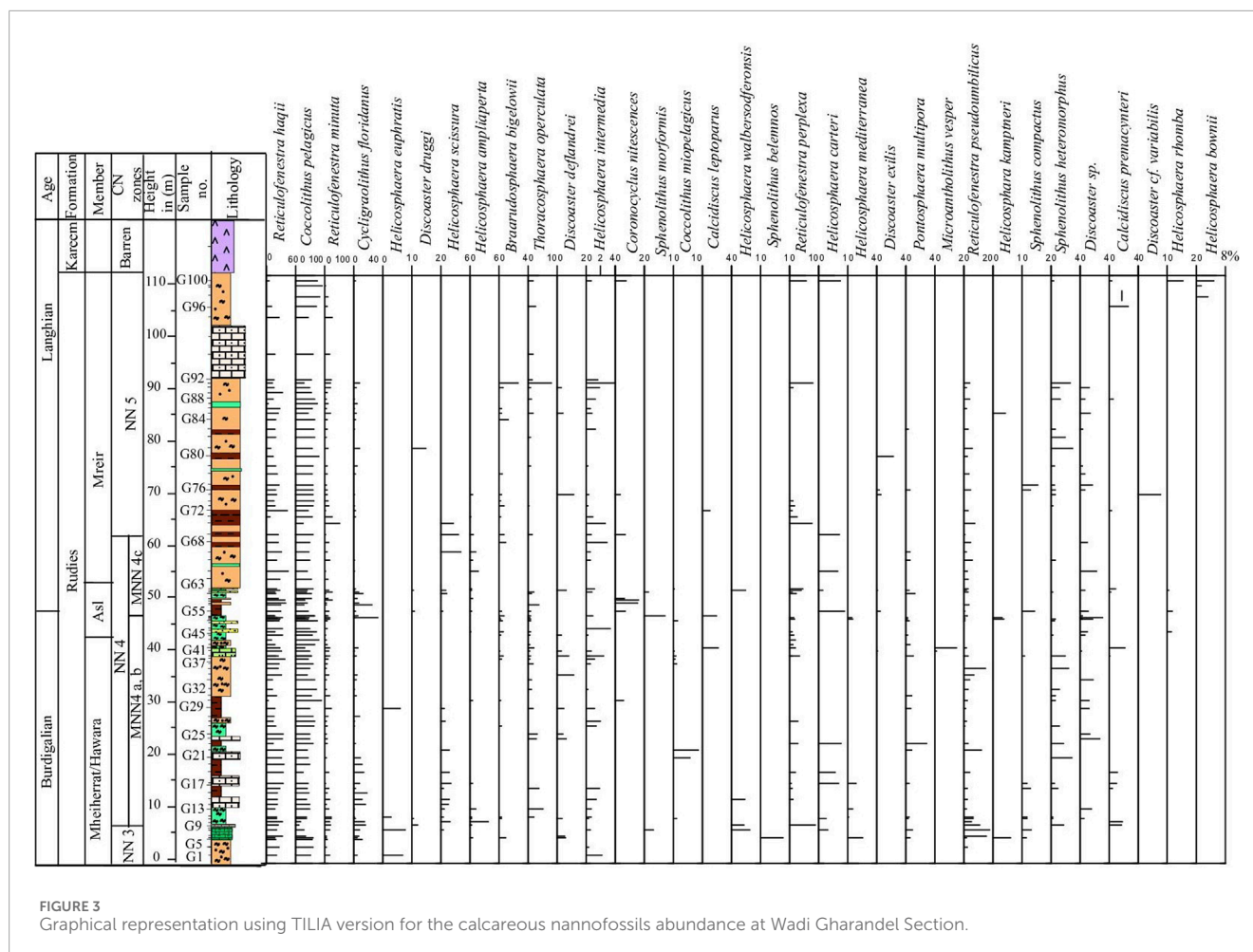


nannofossil event and placed it in the middle part of Zone NN4 (Gartner, 1992; McGonigal, 2004). The FO of *C. premacintyrei* was placed by Boesiger et al. (2017) at 17.8 Ma, near the base of NN4. In the studied sections, *C. premacintyrei* is recorded at the lower part of NN4. The FO of *Helicosphaera walbersdorferensis* occurs close to the FO of *S. heteromorphus* (Theodoridis, 1984). *Discoaster exilis* is recorded at the upper part of NN4 Zone and is used as a marker to this interval. It is first recorded at sample 116 at Wadi Baba and at Sample G 55 at Wadi Gharandel. *Helicosphaera ampliaperta* shows very low and scattered abundance during the end of its stratigraphic range and may show an expanded range by reworking (Fornaciari et al., 1996). The LO of *H. ampliaperta* was used by Martini (1971) to define NN4/NN5 and by Okada and Bukry (1980) to define the CN3/CN4 zonal boundary. Di Stefano et al. (2008) segmented the NN4 Zone of Martini (1971) into three subzones (MNN4a, MNN4b, and MNN4c). They defined the top of MNN4a by the last common occurrence of *H. ampliaperta*. In Wadi Baba, the LCO of *H. ampliaperta* is above sample 113 and above sample G 13 at Wadi Gharandel. In the studied sections, it is too difficult to differentiate MNN4a from MNN4b due to the rare abundance and discontinuous appearance of *H. ampliaperta*. However, the MNN4c, defined by Di Stefano et al. (2008) as the interval between the beginning of the *S. heteromorphus* paracme (PB) and the upper interval with the end of the paracme (PE), can be defined in the studied sections. During the early Middle Miocene, *S. heteromorphus* experienced a period of absence or very low abundance, identified as a paracme interval by Fornaciari et al. (1996).

The *S. heteromorphus* Zone (NN5) of Bramlette and Wilcoxon (1967) occupies the period from the LO of *H. ampliaperta* to the LO of *S. heteromorphus*. It attains a thickness about 50 m at Wadi Gharandel and 42 m at Wadi Baba and occurs within the uppermost part of Asl and Mreir members. The NN5 Zone is equivalent to the CN4 Zone of Okada and Bukry (1980) and the CNM7 of Backman et al. (2012). According to Di Stefano et al. (2008), NN5 Zone is subdivided into three subzones (MNN5a, MNN5b and MNN5c). The subdivision is depending on the occurrence of *Helicosphaera waltrans* and the common occurrence of *H. walbersdorferensis*. These events are not recorded in the studied sections. The nannofossil assemblage in this zone is greatly similar to Zone NN4, except for the disappearance of *H. ampliaperta*, the revolution of *Discoaster pansus* and *D. cf. variabilis*, and many integrated forms between *D. exilis* and *D. deflandrei*.

5.2 Nannofossil assemblages

The abundance of important marker nannofossil species is studied (Figures 7, 8). The R-mode cluster analysis, including all the recorded taxa, reveals four group clusters, which are used to classify the assemblage in both Wadi Baba and Wadi Gharandel sections (Figures 9, 10). Group A only corresponds to *C. pelagicus*, which is the most abundant of all the investigated samples. It reaches up to 85% in some samples. Group B includes *R. minuta* and *R. haqii*. The latter species is abundant, and its values reach up to 49%. The



fluctuations of *R. minuta* reach about 30% and show a continuous appearance in the Wadi Gharandel section in reverse to Wadi Baba, which shows a discontinuous appearance. Group C contains *Cyclicargolithus floridanus*, *Reticulofenestra pseudoumbilicus*, and *Reticulofenestra perplexa*. *C. floridanus* is the fourth most abundant species in the assemblage and highly variable. It ranges in abundance from 1% to 36% (Figures 2, 3). *R. pseudoumbilicus* shows abundance ranging from 1% to 17%, with a rarely sharp increase in some samples up to 33%. Group D contains all the taxa that have abundance less than 5%, including all the species of the genera *Helicosphaera*, *Sphenolithus*, *Discoaster*, *Pontosphaera*, *calcidiscus*, *Microantholithus*, *Braarudosphaera*, and *Coronocyclus*. *Sphenolithus heteromorphus* and *Sphenolithus moriformis* are the most abundant in the *Sphenolithus* group. The major species recorded from *Helicosphaera* genera are *H. mediterranea*, *H. ampliaptera*, *Helicosphaera scissura*, and *Helicosphaera intermedia*.

5.3 Diversity

At the Wadi Baba section, species richness (S) varies from 3 to 19 species per sample (Figure 11). Samples 111 and 116 have the most taxa, while samples 80, 109, 120, 121, and 155 have the

fewest (up to three taxa). Species richness varies throughout the section and increases in the lower part of the section within the Mheiherat/Hawara Member, at the contact with the Asl Member, and in the lower and middle parts of the Mreir Member. The Shannon-Wiener diversity index ranges from 0.4 to 1.8. The dominance index in the studied section contains values from 0.2 to 1. At the Wadi Gharandel section, the species richness ranges from 3 to 17 species per sample (Figure 12). It shows an increase in the middle part of the Mheiherat/Hawara Member, within the Asl Member, and in the lower middle part of the Mreir Member. The Shannon index shows values from 0.5 to 1.9, whereas the dominance ranges from 0.1 to 0.9.

6 Discussion

6.1 The calcareous nannofossil bioevents across the Burdigalian/Langhian (B/L) boundary

There is no particular global stratotype section for the Burdigalian and Langhian stages (Turco et al., 2011; Agnini et al., 2017). The Submission of the Neogene Stratigraphy (SNS) specified three sections as GSSP for the Langhian stage (Lavoda section in

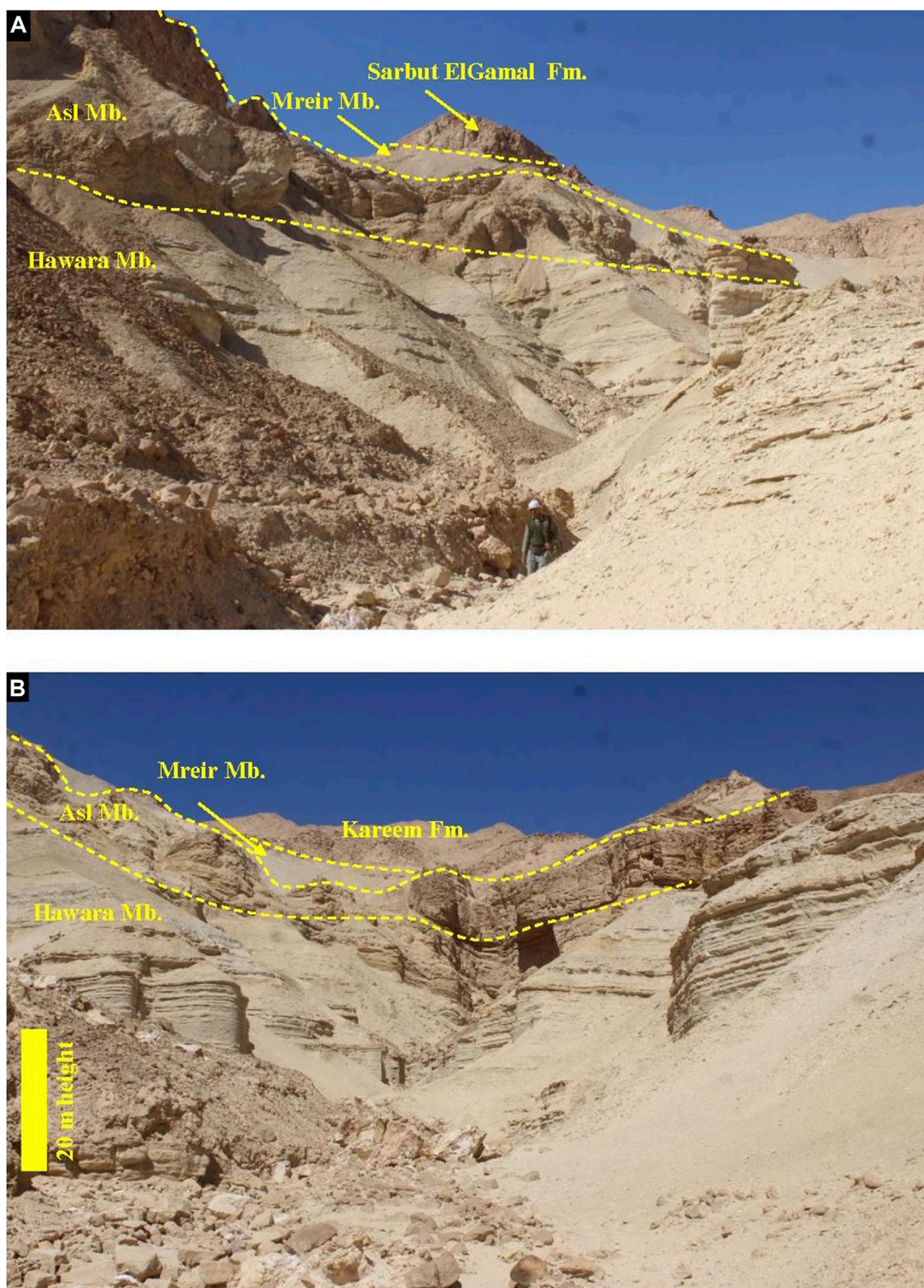


FIGURE 4
(A) The contact between Hawara, Asl and Mreir members at Wadi Baba section. **(B)** The contact between Hawara, Asl and Mreir members at Wadi Gharandel section.

Italy, Atlantic site DSDP 608, and Malta sections). Many authors used the microfossils as a biostratigraphic tool for the Langhian stage and to specify the bioevents across the boundary in the three GSSP sections (e.g., [Di Stefano et al., 2008](#) in Atlantic site DSDP 608

and other sections in the Mediterranean area; [Aziz et al., 2008](#) in the Mediterranean area; [Turco et al., 2011](#) in the Lavoda section). The following are the calcareous nannofossil bioevents across the B/L boundary.

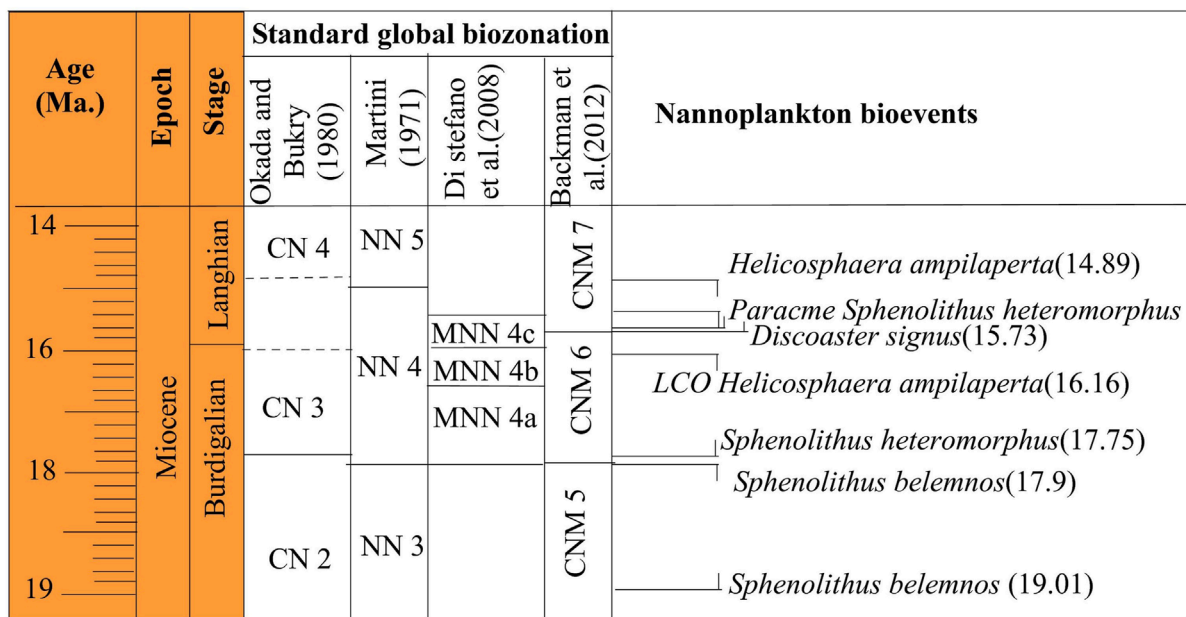


FIGURE 5
Calcareous nannofossil biozonation and bioevents across the Burdigalian and Langhian stages.

Firstly, to define the top of the CN3 Zone, Okada and Burky (1980) used the top acme end of *Discoaster deflandrei* as a marker. This event is not noticed in the studied sections due to the low abundance and scarcity of the species. The end-acme event of *D. deflandrei* was tested in many sections in Mediterranean and oceanic areas, detecting its poor value as a marker (Fornaciari et al., 1990; Rio et al., 1990; Fornaciari et al., 1996; Di Stefano et al., 2008). The lowest occurrence of the *Discoaster exilis* group was used by Martini and Worsley (1970) to convergent the Burdigalian/Langhian boundary. This bioevent is registered in the two studied sections. The FO of *Discoaster exilis* in the Wadi Baba section is in sample 116 and in sample G55 in the Wadi Gharandel section. Ciommelli et al. (2017) recorded many transitional forms between *D. exilis* and *D. signus*, *Discoaster deflandrei* and *D. exilis*, and *Discoaster variabilis* and *D. exilis* occurring within the Burdigalian/Langhian boundary. Many transitional forms of the *D. exilis* group and *D. deflandrei* group, as well as *D. cf. variabilis*, are observed in samples G 55 to G 75 in the Wadi Gharandel section and from samples 116 to 139 in Wadi Baba, indicating the Langhian. The FO of *D. petaliformis* was recorded at 15.778 Ma (De Kaenel et al., 2017; Chakraborty et al., 2021), and used as a marker for the beginning of the Langhian stage. The present study recorded the species in the Wadi Baba section, indicating the Langhian stage.

Second, during the early middle Miocene, *S. heteromorphus* experienced a period of absence or very low abundance identified as a paracme interval by Fornaciari et al. (1996). He recorded this event in Mediterranean Langhian sections. Di Stefano et al. (2008) placed the lower interval of MNN4c with the beginning of the *S. heteromorphus* paracme (PB) and the upper interval with the end of the paracme (PE). This event is recorded at the beginning of the middle Miocene (Langhian) in the two studied sections. The B/L

boundary is noted at the basal part of the Asl Member at the Wadi Gharandel section.

From the previous bio events, the B/L boundary occurred at the basal part of Asl Member at Wadi Baba and Wadi Gharandel. These results contrast with the study of Hewaidy et al. (2013), as the boundary is placed between Asl and Mreir members.

6.2 Paleocological interpretation

The nannofossil abundance, diversity, and cluster analysis are used to explain the paleocological changes in the studied sections. The R-mode cluster analysis shows four distinct groups with different paleocological preferences (Groups A, B, C, and D).

Group A includes just *Coccolithus pelagicus*. This species is adapted to the cool nutrient-rich water conditions, where temperatures range from -1.7°C to 15°C (e.g., McIntyre and Bé, 1967; Okada and McIntyre, 1979; Cachao and Moita, 2000). In Miocene, *C. pelagicus* is present in both cool and tropical conditions as it changes the inhabitant from time to time (Chakraborty et al., 2021).

Group B includes two types of reticulofenestrids (*R. minuta* and *R. haqii*). *R. minuta* indicates stable water conditions and terrigenous nutrient inputs (Wade and Bown, 2006), whereas *R. haqii* prefers warm conditions but can also thrive under temperate water conditions (Haq, 1980). Small Reticulofenestra display an opportunistic behaviour during episodes of high fertility (Okada, 2000) or in zones of upwelling (Okada and Wells, 1997). The dominance of these taxa in Neogene sediment indicates mesotrophic-eutrophic surface water conditions (Okada, 2000; Takahashi and Okada, 2000; Krammer et al., 2006). In the present work, *R. haqii* is considered to have a mesotrophic affinity,

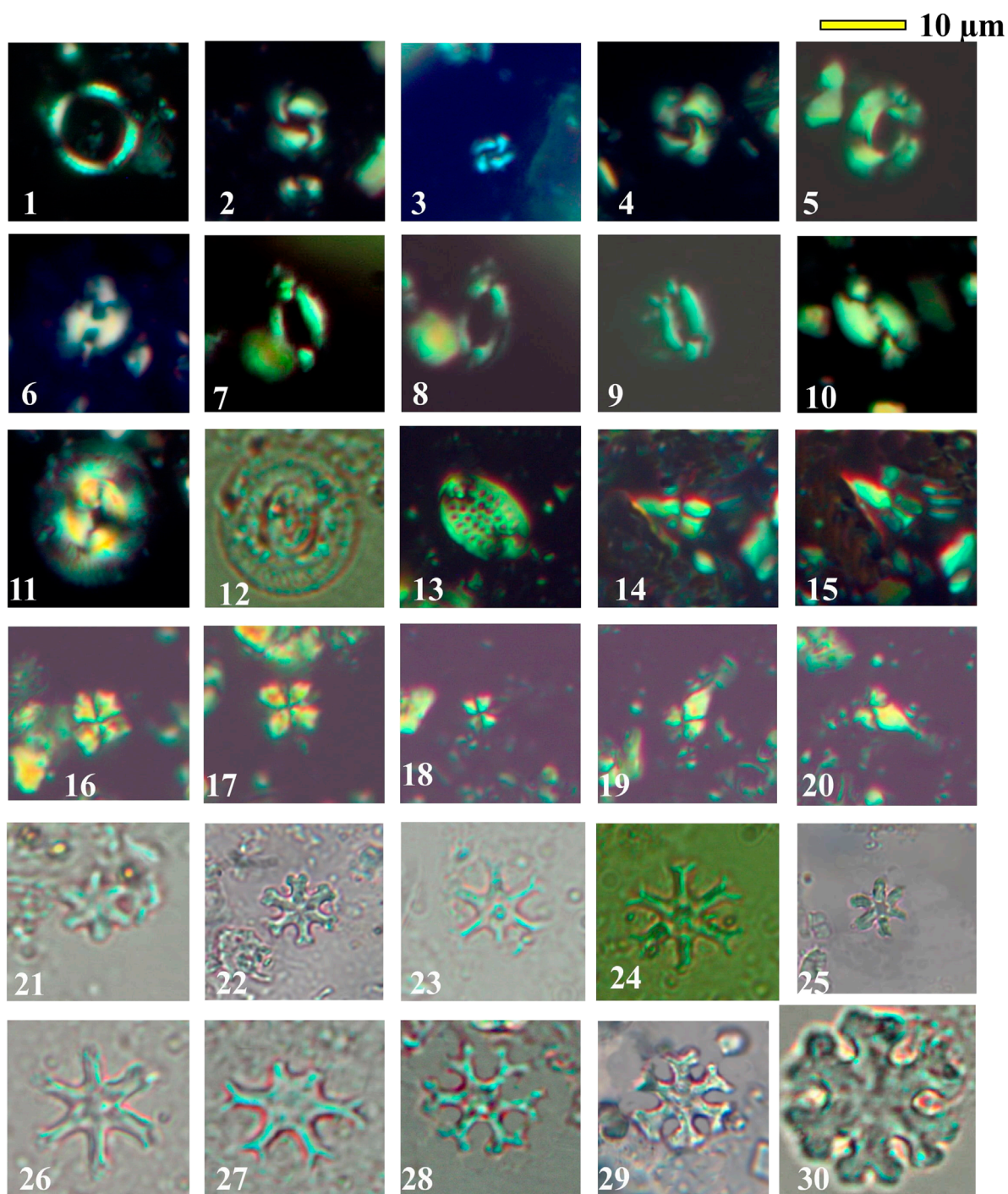


FIGURE 6

1- *Coronocyclus nitescens*. Sample No. G99, Wadi Gharandel. 2. *Reticulofenestra haqii*. Sample No. 106, Wadi Baba 3- *Reticulofenestra minuta*. Sample No. G29, Wadi Gharandel. 4- *Calcidiscus premacynteri*. Sample No. 128, Wadi Baba. 5- *Reticulofenestra pseudumbilicus*. Sample No. 130, Wadi Baba. 6- *Helicosphaera mediterranea*. Sample No. 48, Wadi Baba. 7, 8- *Helicosphaera ampliaperta*. Sample No. G45, Wadi Gharandel. 9- *Helicosphaera scissura*. Sample No. 116, Wadi Baba. 10- *Helicosphaera carteri*. Sample No. 144, Wadi Baba. 11, 12- *Coccolithus miopelagicus*. Sample No. 146, Wadi Baba. 13- *Pontosphaera multipora*. Sample No. 127, Wadi Baba. 14, 15- *Sphenolithus belemnus*. Sample No. 91, Wadi Baba. 16, 17- *Sphenolithus morformis* Sample No. 157, Wadi Baba. 18, 19, 20- *Sphenolithus heteromorphus*. Sample No. 153, Wadi Baba. 21- *Discoaster druggii*. Sample No. 136, Wadi Baba. 22- *Discoaster deflandrei*. Sample no. 116, Wadi Baba. 23, 24- *Discoaster cf. variabilis*. 23- Sample no.G75, 24- Sample No. G 55, Wadi Gharandel section. 25- *Discoaster petaliformis*. Sample no. 128, Wadi Baba. 26- Integrating from *Discoaster exilis*-*Discoaster variabilis*. Sample no. G 75, Wadi Gharandel. 27- *Discoaster exilis*. Sample no. 116, Wadi Baba. 28, 29- *Discoaster pansus*. Sample no. 131, Wadi Baba. 30- *Discoaster deflandrei*. Sample No. 116, Wadi Baba.

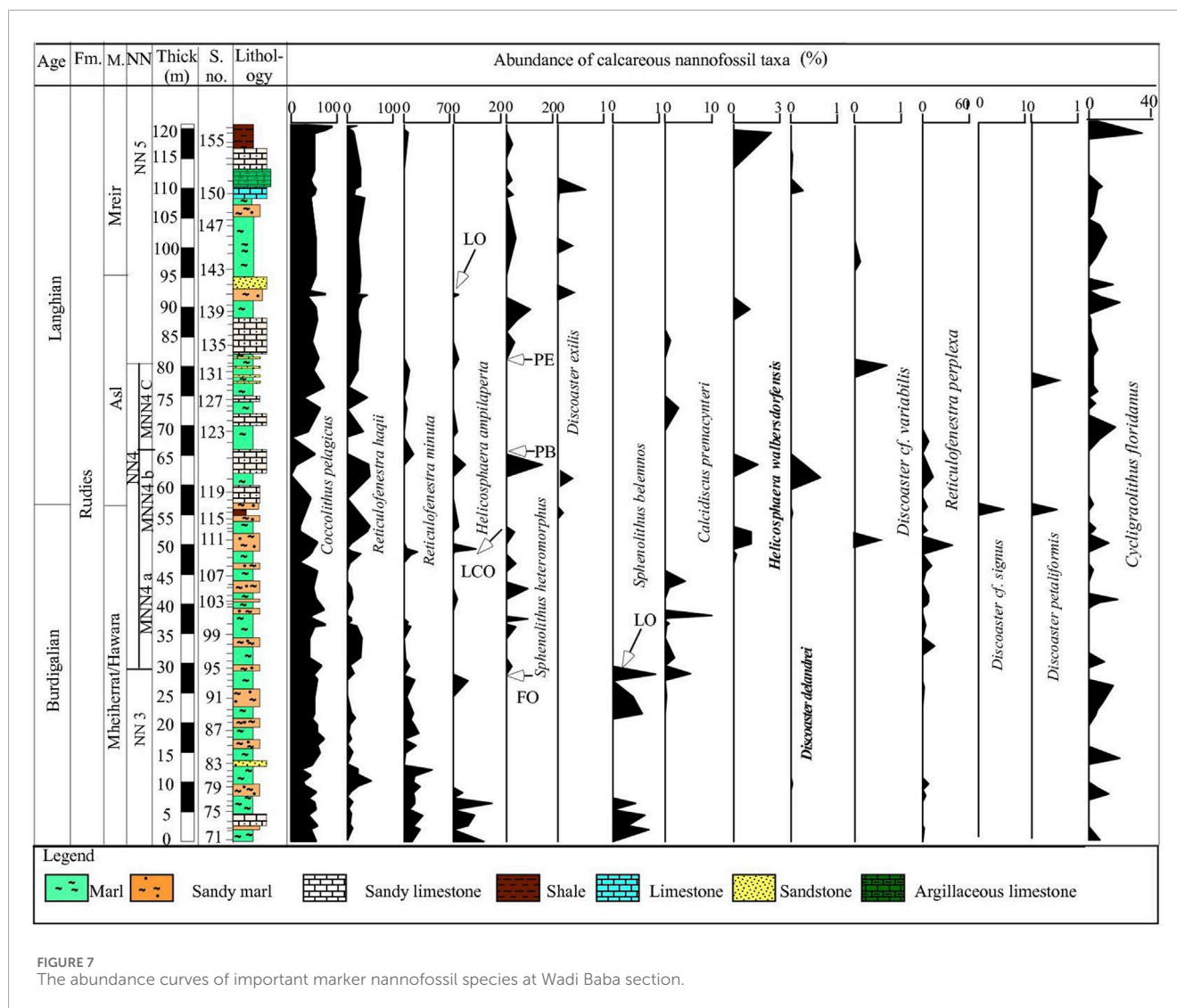


FIGURE 7
The abundance curves of important marker nannofossil species at Wadi Baba section.

depending on the positive correlation between this species and the mesotrophic *R. minuta*. Small reticulofenestrids also indicate upwelling conditions (Chakraborty et al., 2021; Chakraborty et al., 2023) and are present in modern upwelling regions (Takahashi and Okada, 2000).

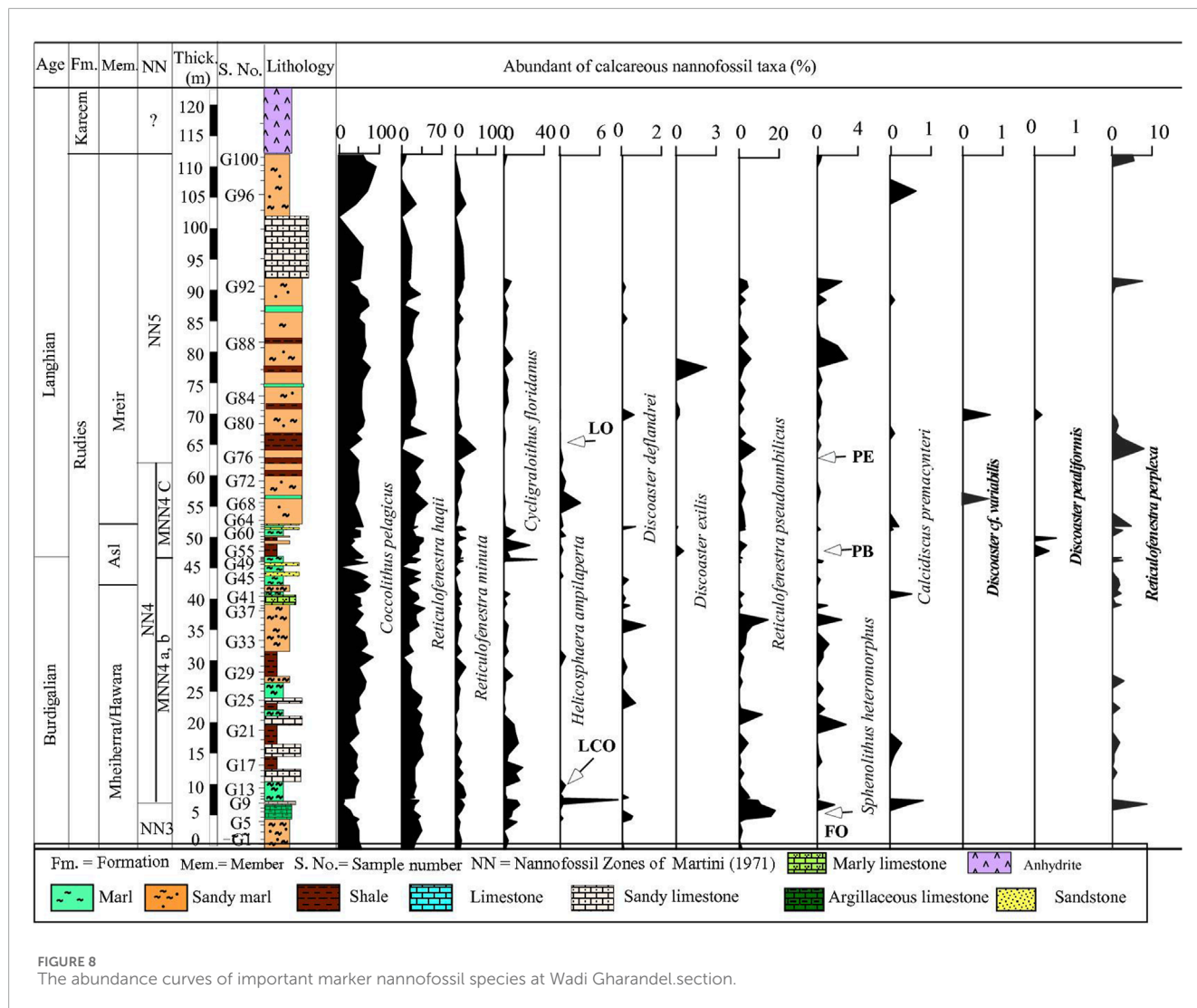
Group C consists of three taxa: *C. floridanus*, *R. pseudoumbilicus*, and *R. perplexa*. The cosmopolitan *C. floridanus* (Wei and Wise, 1990) is interpreted as a long-ranging species found in a wide range of latitudes and is a eutrophic species (Aubry, 1992; Monechi et al., 2000). *R. perplexa* exhibits a strong preference for high latitudes and cooler water conditions (Haq, 1980; Wei and Wise, 1990; McGonigal, 2004). *R. pseudoumbilicus* is indicative of high nutrient levels (Lohmann and Carlson, 1981).

Group D includes all the species whose abundance is less than 7%. It contains *Helicosphaera*, *Pontosphaera*, *Sphenolithus*, and *Discoaster*. *Sphenolithus* and *Discoaster* are related to the same paleoecological interpretation (Haq, 1980; Wei and Wise, 1990). *Discoaster* has been interpreted as a warm-water genus (Bukry, 1973), whereas *Sphenolithus* prefers warm, oligotrophic conditions (Bralower, 2002). Villa and Persico (2006) treated *Sphenolithus* as

warm-water taxa in their studies of Oligocene sediments from the Indian Ocean. *Helicosphaera* spp. are recorded in the regressive phases of siliclastic margins (De Kaenel and Villa, 1996). Helicosphaerids are interpreted to adapt to hemipelagic settings (Aubry, 1990; Ziveri et al., 1995). These species are more commonly found in tropical to subtropical assemblages and are rarely recorded in temperate to subarctic assemblages (Chira and Malacu, 2008). Peaks in *Helicosphaera* spp. are recorded in the regressive phases of siliclastic margins (De Kaenel and Villa, 1996).

6.3 Biotic responses to sea-level changes

Generally, the Miocene was an interval of highly instability in climate and highly variable between cool and warm periods (Jovane et al., 2019; Jovane et al., 2020). In the present study, the fluctuations in nannofossil assemblages and abundance of the early-middle Miocene Rudies Formation at Wadi Baba and Wadi Gharandel sections indicate paleoecological changes during this period of time. The cool and temperate water taxa such as *C. pelagicus*, *R. haqii*, and *R. minuta* are the dominant assemblage in the Mheiherratt/Hawara Member. In this interval, approximately



similar values of the Shannon index indicate stable water conditions. The taxa *R. haqii* and *R. minuta* are thought to be representative of nutrient-rich waters with little variations in nutrient availability, temperature, or turbulence in the surface water (Auer et al., 2014). Although the abundance of both *R. minuta* and *R. haqii* are relatively smaller than that of *C. pelagicus* in the lower part of the Mheiherrat/Hawara Member, a sudden increase took place for these small reticulofenestrads relative to *C. pelagicus* from sample 79 to sample 82 (Figure 7). The higher percentage of small reticulofenestrads indicates high terrigenous inputs (Aubry, 1992; Persico and Villa, 2004; Chakraborty et al., 2021). Therefore, shallowing conditions and sea-level falling episodes are suggested and may match the Bur3 boundary of Hardenbol et al. (1998). In summary, this interval is characterized by a slight sea-level rise followed by a sudden drop in the sea-level at the end of this interval. At the topmost part of this interval, there is a transition from a more stable marine to a shallower depositional environment with freshwater influence.

The second part encompasses the middle and upper parts of Mheiherrat/Hawara Member. This interval contains a higher percentage of *C. pelagicus* and the open-water species *C. floridanus*, with a lower percentage of small reticulofenestrads relative to the first interval (Figure 7). It indicates more deep marine, cooler water conditions, and more distance from the shore. Again, near the top of Mheiherrat/Hawara Member, small fluctuations in sea-level conditions and a slight sea-level fall could be induced due to the increase in small reticulofenestrads and a slight decrease in *C. pelagicus*. There is a sudden decrease in *C. pelagicus* from 66% to 20% in sample 110 and a sudden increase in *R. perplexa* up to 45% (Figure 7). The relative increase of *C. pelagicus* and *R. perplexa* is used to indicate surface water cooling during the Miocene (Wei and Wise, 1992).

The third interval (samples 116–122) comprises the lower part of the Asl Member and includes the middle part of the NN4 Zone and the interval of the B/L boundary. This interval contains many barren intervals and is characterized by a decrease in *C. pelagicus*

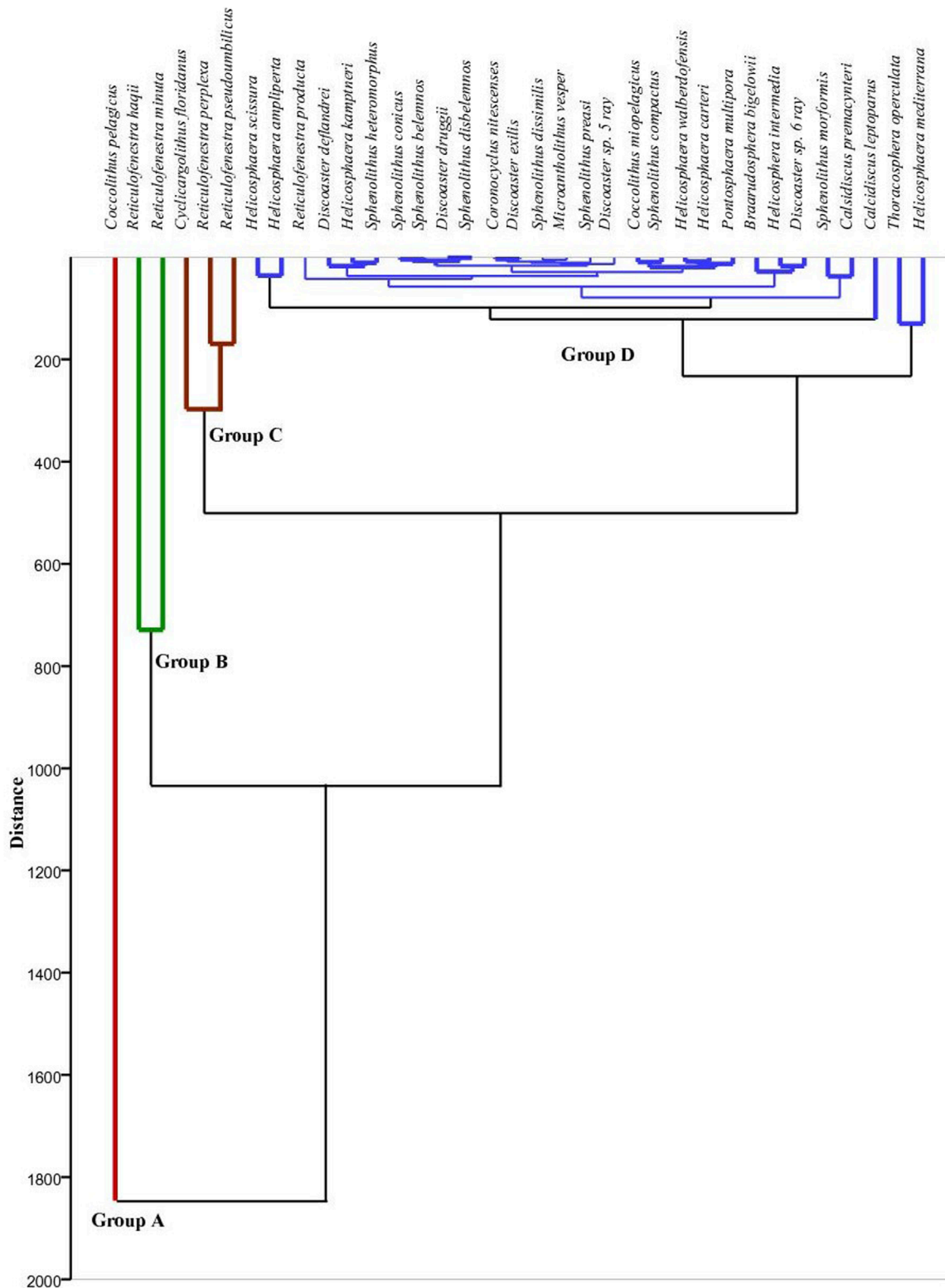


FIGURE 9 R-mode cluster analysis of nannofossil assemblages using Ward's method at Wadi Baba section.

and an increase in *R. haqii* with an increase in the Shannon-Weiner diversity index (Figure 11). This indicates more proximity to the shore with warm water conditions (Figure 11). The common *R.*

haqii, followed by *C. pelagicus*, indicates a nearshore nutrient-rich environment and points to warmer stratified (stressed) waters with reduced upwelling (Auer et al., 2014; Jamrich et al., 2024).

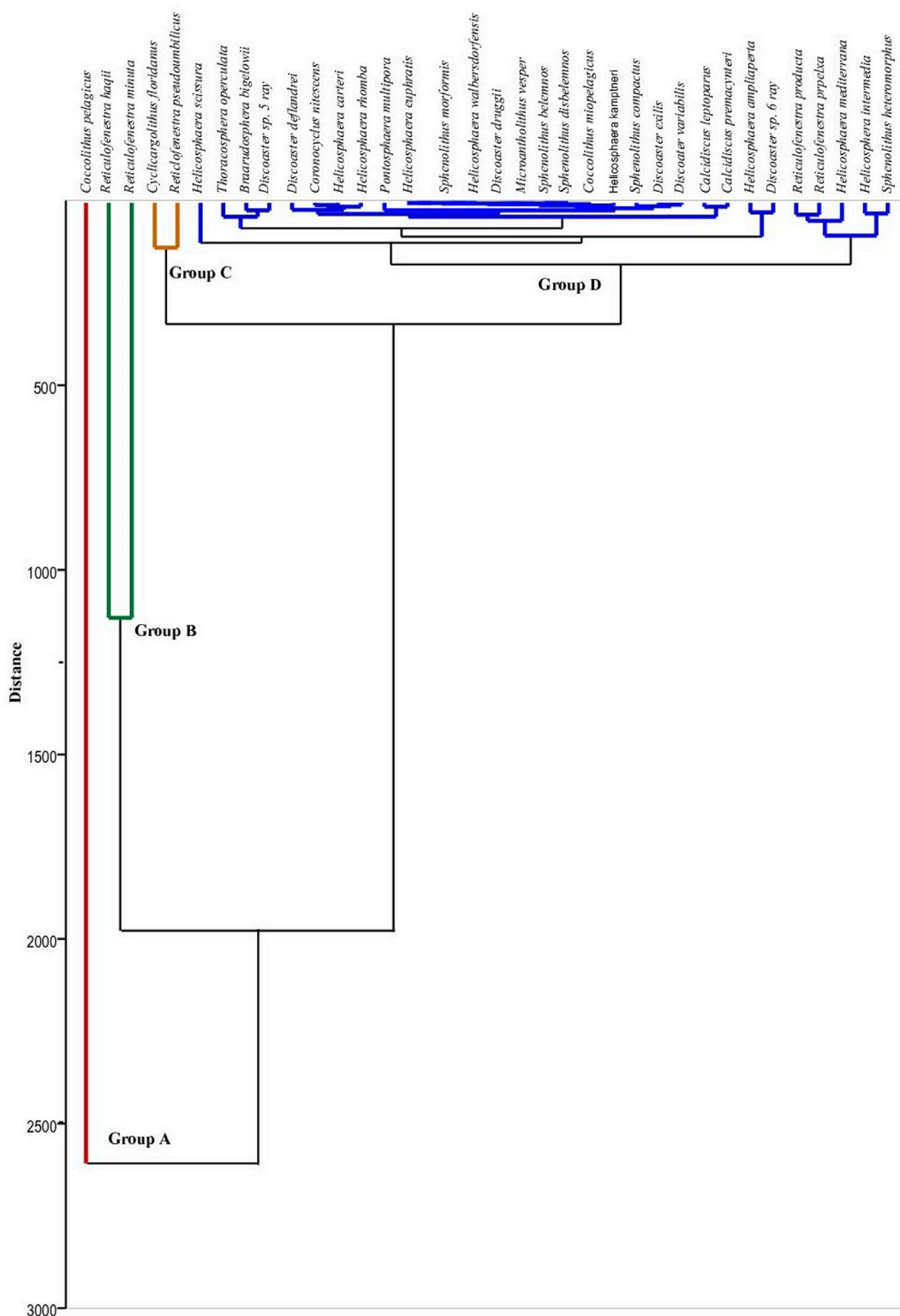


FIGURE 10 R-mode cluster analysis of nannofossil assemblages using Ward's method at Wadi Gharandel section.

The fourth interval includes the majority of the Asl Member and the Mreir Member. This interval is generally characterized by the lowest abundance and discontinuous appearance of *R.*

minuta. In most samples, *C. pelagicus* is high in abundance, except in some samples, which indicate small fluctuations in sea-level. This interval shows the same conditions as those in the second

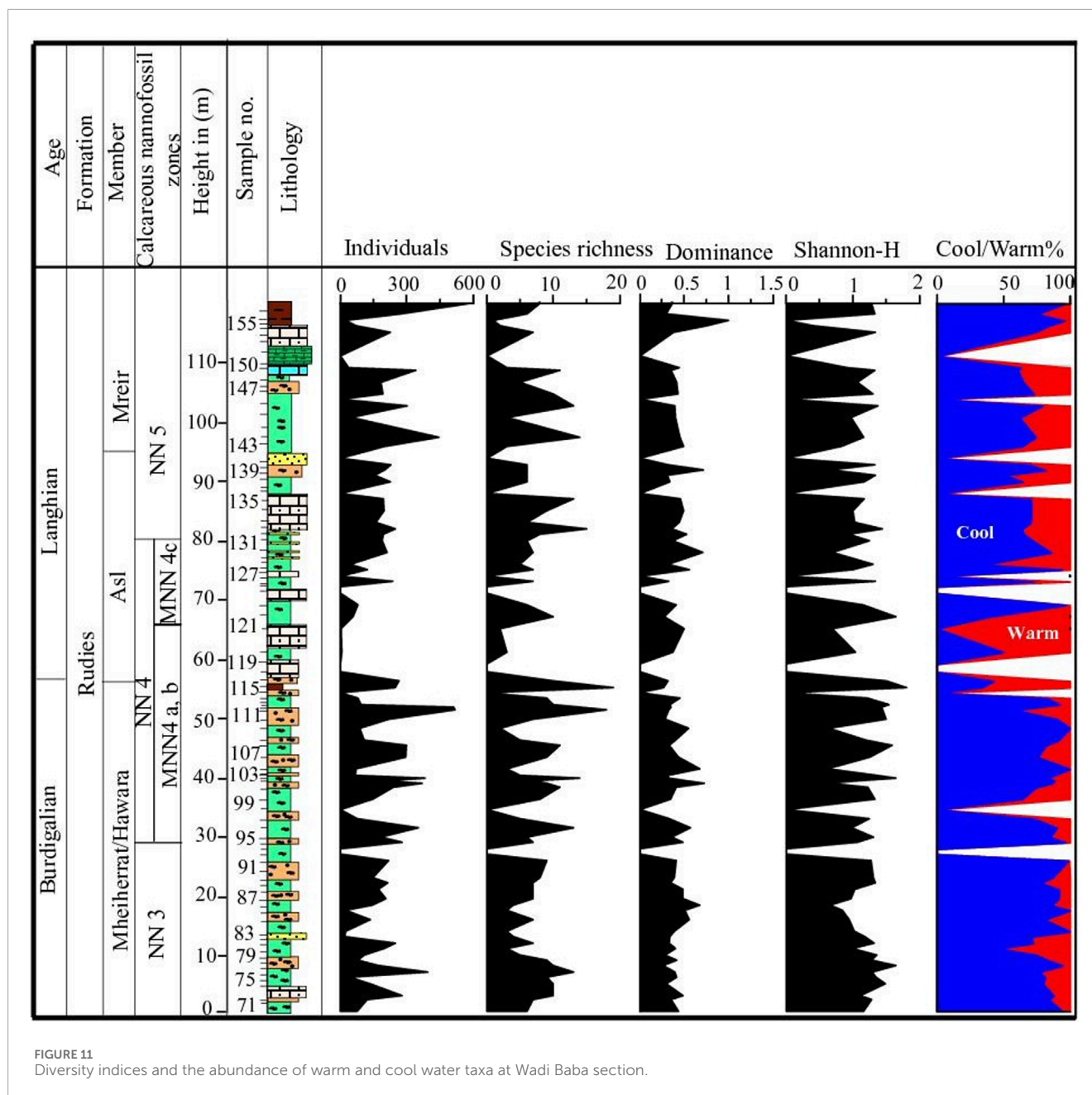


FIGURE 11 Diversity indices and the abundance of warm and cool water taxa at Wadi Baba section.

interval, as well as small fluctuations similar to those in the third interval, which indicate a rise in sea-level and cool water conditions with small sea-level changes (slight falling) in samples 129 and 139.

At Wadi Gharandel, the first interval (samples G1 to G10) has similar conditions to the Wadi Baba lower interval. The *C. pelagicus* abundance declines at the top of this interval, with increasing abundance of small reticulofenestrads indicating proximity to the shore with a transition from cool water to warm water conditions. This may contradict Bur3 of Hardenbol et al. (1998). The second interval comprises the most Mheiherratt/Hawara Member (samples G11 to G31). It is characterized by a moderate abundance of *C. pelagicus* and small reticulofenestrads, indicating shelf marine conditions. The third interval includes the most

Asl and the lowest part of Mreir members (samples G32 to G54). *C. pelagicus* became more abundant relative to small reticulofenestrads, indicating deeper marine conditions with small fluctuations in sea-level. At the B/L boundary, there is a turnover in the ecology to warm water conditions and a sudden decrease in *C. pelagicus* (samples from G55–G58) (Figure 12). In the Gharandel section, a strong drop in *C. pelagicus* is accompanied with an increase in small- and medium-sized reticulofenestrads and *C. floridanus* is noted across the B/L boundary (Figure 12). According to Auer et al. (2014), such an arrangement suggests less water turbulence and upwelling. The next interval occurs within Mreir Member and has alternating conditions and many fluctuations similar to the second and third intervals.

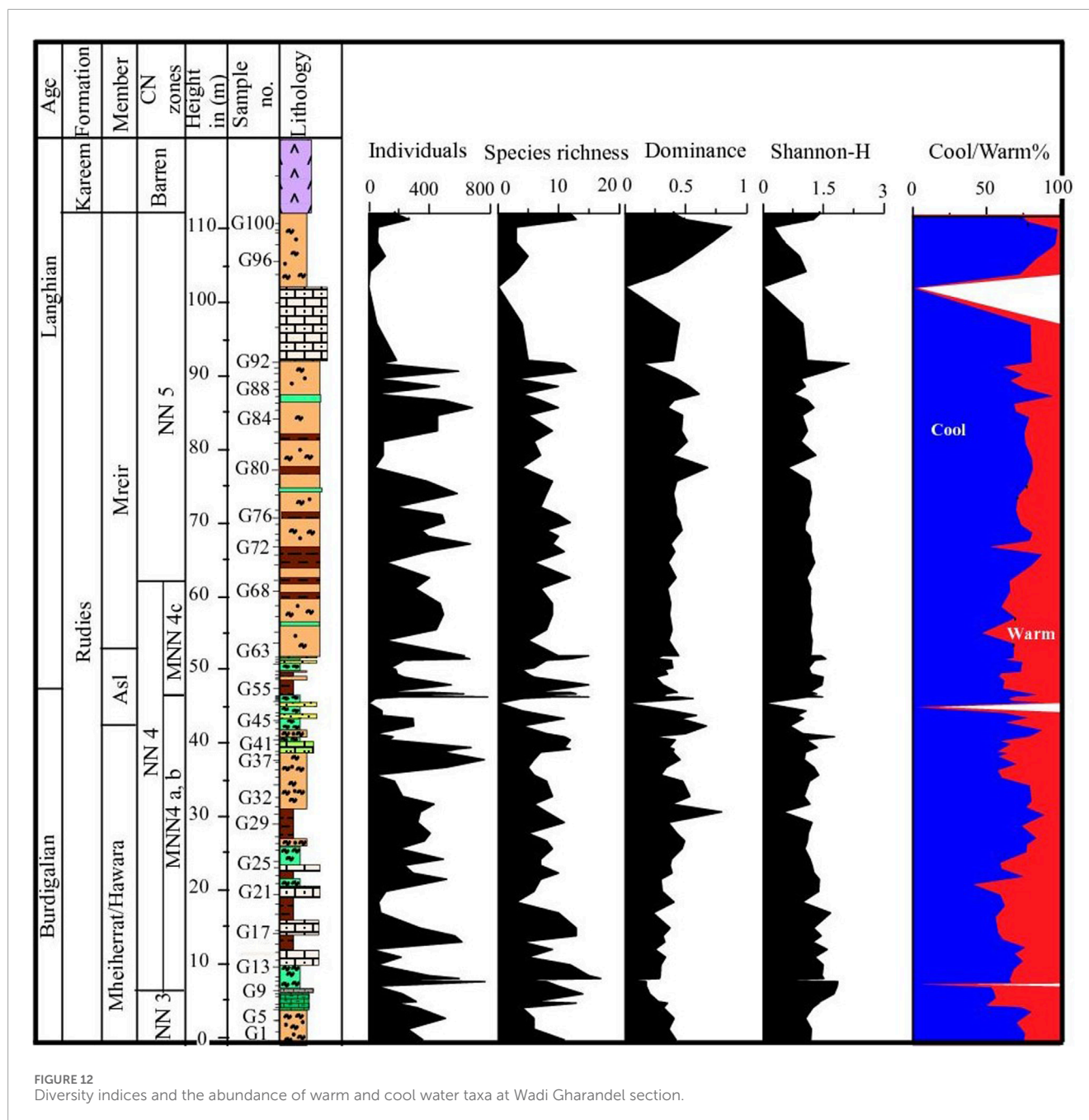


FIGURE 12
Diversity indices and the abundance of warm and cool water taxa at Wadi Gharandel section.

7 Conclusion

This study attempts to provide detailed calcareous nannofossil bioevents and palaeoecological interpretation across outcrops of the Burdigalian-Langhian succession on the eastern margin of the Gulf of Suez. Lithostratigraphically, the Burdigalian-Langhian succession in the study area is represented by the Rudies Formation, which can be subdivided into three members from base to top: Mheiherrat/Hawara, Asl, and Mreir; respectively. Biostratigraphically, the sediments were dated and included in three biozones (NN3, NN4, and NN5). The study provides an age refinement for the three members of the Rudies Formation whereas the Mheiherrat/Hawara Member corresponds to the Burdigalian

stage, represented by the *S. belemnus* NN3 Zone and the lower part of the *S. heteromorphus* NN4 Zone. The B/L boundary is placed at the base of the Asl Member in both the Wadi Baba and Wadi Gharandel sections. The major bioevents used to define this boundary include the evolution of the *Discoaster exilis* group, the transitional forms between *D. exilis* and *D. variabilis*, the absence interval of *S. heteromorphus* (the paracme interval) and the occurrence of *D. petaliformis*. The NN4/NN5 zonal boundary is situated within the Mreir Member at the Wadi Gharandel section and within the Asl Member at the Wadi Baba section, based on the LO of *H. ampliapertura* and the PE of *S. heteromorphus*. Cluster analysis groups the nannofossil species into four aggregations that reflect their related ecological preferences. The most abundant taxa

in the assemblage are *C. pelagicus* as well as *R. haqii*, *R. minuta*, and *C. floridanus*. The overall condition was nutrient-rich, cooler water. The final intervals show high sea-level conditions with minor fluctuations and a slight decline in sea level. The biotic response to sea-level changes is discussed based on fluctuations in species abundance. Generally, the first interval indicates a slight rise in sea level, followed by a sudden drop at the end of the interval. The fluctuations in nannofossil abundance during the second interval suggest a greater distance from the shore with more open marine conditions. During the third interval, sea level fell, marking the contact between the Asl and Hawara members at the B/L boundary. The final intervals show high sea-level conditions with minor fluctuations accompanied by a slight decline in sea level.

Data availability statement

The raw data supporting the conclusions of this article will be made available by the authors, without undue reservation.

Author contributions

AA: Conceptualization, Data curation, Formal Analysis, Investigation, Methodology, Software, Supervision, Writing—original draft, Writing—review and editing. SE-N: Conceptualization, Data curation, Formal Analysis, Investigation, Methodology, Software, Visualization, Writing—original draft, Writing—review and editing. SF: Conceptualization, Data curation, Formal Analysis, Investigation, Methodology, Software, Supervision, Writing—original draft, Writing—review and editing. LJ: Conceptualization, Formal Analysis, Funding acquisition, Investigation, Methodology, Resources, Software, Writing—review and editing. KA-K: Conceptualization, Formal Analysis, Funding acquisition, Investigation, Methodology, Writing—review and editing. AZ: Conceptualization, Formal Analysis, Funding acquisition, Methodology, Writing—review and editing, Investigation, Resources, Software, Writing—original draft.

Funding

The author(s) declare that financial support was received for the research, authorship, and/or publication of this article. LJ and CORE

References

- Abul-Nasr, R., and Salama, G. (1999). Paleocology and depositional environments of the Miocene rocks in western Sinai, Egypt. Middle east research center. *Ain Shams Univ. Earth Sci. Ser.* 13, 92–134.
- Agnini, C., Monechi, S., and Raffi, I. (2017). Calcareous nannofossil biostratigraphy: historical background and application in Cenozoic chronostratigraphy. *Lethaia* 50 (3), 447–463. doi:10.1111/let.12218
- Alsharhan, A. S. (2003). Petroleum geology and potential hydrocarbon plays in the Gulf of Suez rift basin, Egypt. *Am. Assoc. Pet. Geol. Bull.* 87 (1), 143–180.
- Andrawis, S. F., and Abdel Malik, W. M. (1981). Lower/middle Miocene boundary in Gulf of Suez region, Egypt. *Newsl. Stratigr.* 10, 156–163. doi:10.1127/nos/10/1981/156
- Aubry, M.-P. (1990). Handbook of cenozoic calcareous nannoplankton-book 4 heliolithae (helicoliths, cribriliths, lopadoliths and others): micropaleontology press. *Am. Mus. Nat. Hist.* 381pp.
- Aubry, M.-P. (1992). “Late Paleogene calcareous nannoplankton evolution: a tale of climatic deterioration,” in *Eocene-oligocene climatic and biotic evolution*. Editors D. R. Prothero, and W. A. Berggren (New Jersey: Princeton University Press), 272–208.
- Auer, G., Piller, W. E., and Harzhauser, M. (2014). High-resolution calcareous nannoplankton palaeoecology as a proxy for small-scale environmental changes in the Early Miocene. *Mar. Micropaleontol.* 111, 53–65. doi:10.1016/j.marmicro.2014.06.005
- Ayyad, H. M., Fathy, M., Hewaidy, A. G. A., and Abdallah, A. (2020). Sequence stratigraphy of the burdigalian Rudeis Formation in ras el-ush oil field, Gulf of Suez:

lab are supported by Fundação de Amparo à Pesquisa do Estado de São Paulo (FAPESP) project 2016/24946-9. AZ is also supported by FAPESP grant number 2022/08285-3.

Acknowledgments

The authors would like to express their sincere gratitude to the two reviewers and the handling editor of *Frontiers in Earth Science* for their valuable feedback and insightful comments. Their constructive critiques have significantly enriched our manuscript and contributed to its improvement. KA-K also acknowledges the Research Supporting Project Number RSP 2024R139, King Saud University (Riyadh, Saudi Arabia) for its support.

Conflict of interest

The authors declare that the research was conducted in the absence of any commercial or financial relationships that could be construed as a potential conflict of interest.

The author(s) declared that they were an editorial board member of *Frontiers*, at the time of submission. This had no impact on the peer review process and the final decision.

Publisher's note

All claims expressed in this article are solely those of the authors and do not necessarily represent those of their affiliated organizations, or those of the publisher, the editors and the reviewers. Any product that may be evaluated in this article, or claim that may be made by its manufacturer, is not guaranteed or endorsed by the publisher.

Supplementary material

The Supplementary Material for this article can be found online at: <https://www.frontiersin.org/articles/10.3389/feart.2024.1442241/full#supplementary-material>

- application of gamma-ray analysis and biostratigraphy. *Mar. Pet. Geol.* 122, 104694. doi:10.1016/j.marpetgeo.2020.104694
- Ayyad, H. M., Hewaidy, A. G. A., and Al-Labaidy, N. A. (2022). Sequence stratigraphy of the Miocene siliciclastic-carbonate sediments in sadat area, north-west of Gulf of Suez: implications for Miocene eustasy. *Geol. J.* 57 (6), 2255–2270. doi:10.1002/gj.4406
- Aziz, H. A., Di Stefano, A., Foresi, L., Hilgen, F. J., Iaccarino, S., Kuiper, K., et al. (2008). Integrated stratigraphy and ⁴⁰Ar/³⁹Ar chronology of early middle Miocene sediments from DSDP leg 42A, site 372 (western mediterranean). *Palaeogeogr. Palaeoclimatol. Palaeoecol.* 257 (1–2), 123–138. doi:10.1016/j.palaeo.2007.09.013
- Backman, J., Raffi, I., Rio, D., Fornaciari, E., and Pälke, H. (2012). Biozonation and biochronology of Miocene through Pleistocene calcareous nannofossils from low and middle latitudes. *Newsletters Stratigr.* 45 (3), 221–244. doi:10.1127/0078-0421/2012/0022
- Bergen, J. A., Truax III, S., De Kaenel, E., Blair, S., Browning, E., Lundquist, J., et al. (2019). BP Gulf of Mexico Neogene astronomically-tuned time scale (BP GNATTS). *Bulletin* 131 (11–12), 1871–1888. doi:10.1130/b35062.1
- Boesiger, T., De Kaenel, E., Bergen, J., Browning, E., and Blair, S. (2017). Oligocene to Pleistocene taxonomy and stratigraphy of the genus *Helicosphaera* and other placolith taxa in the circum North Atlantic Basin. *J. Nannoplankt. Res.* 37 (2–3), 145–175. doi:10.58998/jnr2021
- Bosworth, W., Crevello, P., Winn, R. D., and Steinmetz, J. (1998). “Structure, sedimentation, and basin dynamics during rifting of the Gulf of Suez and northwestern Red Sea,” in *Sedimentation and tectonics of rift basins: red sea-gulf of aden*. Editors B. H. Purser, and D. W. J. Bosence (London: Chapman & Hall), 77–96.
- Bosworth, W., and McClay, K. (2001). Structural and stratigraphic evolution of the Gulf of Suez rift, Egypt: a synthesis. *Mémoires du Muséum national d’histoire naturelle* (1993), 186, 567–606.
- Boukhary, M., Abd El Naby, A., Faris, M., and Morsi, A. (2012). Plankton stratigraphy of the early and middle Miocene Kareem and Rudeis formations in the central part of the Gulf of Suez, Egypt. *Hist. Biol.* 24 (1), 49–62. doi:10.1080/08912963.2011.578877
- Bown, P. R., and Young, J. R. (1998). “Techniques,” in *Calcareous nannofossil biostratigraphy*. Editor P. R. Bown (London: Chapman and Hall/Kluwer Academic Publishers), 16–28.
- Bradshaw, C. D. (2021). Miocene climates. *Encycl. Geol.*, 486–496. doi:10.1016/b978-0-12-409548-9.12392-9
- Bralower, T. J. (2002). Evidence of surface water oligotrophy during the Paleocene-Eocene thermal maximum: nannofossil assemblage data from ocean drilling program Site 690, Maud rise, Weddell Sea. *Paleoceanography* 17 (2), 13–11. doi:10.1029/2001pa000662
- Bramlette, M., and Wilcoxon, J. (1967). Middle tertiary calcareous nannoplankton of the cipro region, trinidad, WI. *Tulane Stud. Geol. Paleontol.* 5 (3), 93–131.
- Bukry, D. (1973). “Low latitude coccolith biostratigraphic zonation,” in *Initial reports DSDP*, N. T. Edgar, and J. B. Saunders, (Washington: US Govt. Printing Office), 15, 685–703.
- Cachao, M., and Moita, M. (2000). *Coccolithus pelagicus*, a productivity proxy related to moderate fronts off Western Iberia. *Mar. Micropaleontol.* 39 (1–4), 131–155. doi:10.1016/s0377-8398(00)00018-9
- Chakraborty, A., Ghosh, A. K., Dey, R., Saxena, S., and Mazumder, A. (2019). Record of the Miocene climate Optimum in the northeast Indian ocean: evidence from the microfossils. *Palaeobiodiversity Palaeoenvironments* 99 (2), 159–175. doi:10.1007/s12549-018-0342-3
- Chakraborty, A., Ghosh, A. K., and Saxena, S. (2021). Neogene calcareous nannofossil biostratigraphy of the northern Indian Ocean: implications for paleoceanography and paleoecology. *Palaeogeogr. Palaeoclimatol. Palaeoecol.* 579, 110583. doi:10.1016/j.palaeo.2021.110583
- Chakraborty, A., Ghosh, A. K., Saxena, S., Dey, R., and Roy, L. (2023). “Neogene biostratigraphy and paleoceanography of andaman and nicobar basin: a reappraisal,” in *Stratigraphy & timescales*. Editor M. Montenari (Germany: Elsevier), 8, 121–187. doi:10.1016/bs.sats.2023.08.005
- Chira, C., and Malacu, A. (2008). Biodiversity and paleoecology of the Miocene calcareous nannoplankton from Sibiu area (Transylvania, Romania). *Acta Palaeontol. Romaniae* 6, 17–28.
- Ciummelli, M., Raffi, I., and Backman, J. (2017). Biostratigraphy and evolution of Miocene discoaster spp. from IODP site U1338 in the equatorial pacific ocean. *J. Micropaleontology* 36 (2), 137–152.
- Colleoni, F., De Santis, L., Naish, T. R., DeConto, R. M., Escutia, C., Stocchi, P., et al. (2022). “Past Antarctic ice sheet dynamics (PAIS) and implications for future sea-level change,” in *Antarctic climate evolution* (Germany: Elsevier), 689–768.
- De Kaenel, E., Bergen, J., Browning, E., Blair, S., and Boesiger, T. (2017). Uppermost Oligocene to middle Miocene discoaster and catinaster taxonomy and stratigraphy in the circum north atlantic basin: Gulf of Mexico and ODP leg 154. *J. Nannoplankt. Res.* 37 (2–3), 215–244. doi:10.58998/jnr2077
- De Kaenel, E., and Villa, G. (1996). “Oligocene-Miocene calcareous nannofossil biostratigraphy and paleoecology from the Iberia abyssal plain,” in *Proceeding of the ODP, scientific results 149*. Editors R. B. Whitmarsh, D. S. Sawyer, A. Klaus, and D. G. Masson (College Station, TX: Ocean Drilling Program), 79–145.
- Di Stefano, A., Foresi, L. M., Lirer, F., Iaccarino, S. M., Turco, E., Amore, F. O., et al. (2008). Calcareous plankton high resolution biomagnetostratigraphy for the Langhian of the Mediterranean area. *Riv. Ital. Paleontol. Stratigr.* 114 (1), 51.
- El Ayouy, M. K. (1990). “Petroleum geology,” in *The geology of Egypt*. Editor R. Said (Rotterdam, Brookfield: A.A. Balkema), 567–599.
- El-Azabi, M. H. (1996). “A new suggested stratigraphic level for the Miocene Sarbut El-Gamal Formation in the Gulf of Suez, Egypt; a sedimentologic approach,” in *Third international conference on geology of the arab world* (China: Cairo University), 407–432.
- El-Azabi, M. H. (1997). The Miocene marginal marine facies and their equivalent deeper marine sediments in the Gulf of Suez, Egypt, a revised stratigraphic setting. *Egypt. J. Geol.* 41, 273–308.
- El-Azabi, M. H. (2004). Facies characteristics, depositional styles and evolution of the Syn-rift Miocene sequences in Nukhul-Feiran area, Sinai side of the Gulf of Suez rift basin, Egypt. *Sedimentol. Egypt* 12, 69–103.
- El-Deeb, W., Al-Ashwah, A., and Mandur, M. (2004). Planktonic foraminifera and calcareous nannoplankton biostratigraphy of the lower and middle Miocene sequence in Wadi gharandal, southwest Sinai, Egypt. *Egypt. J. Pet.* 13 (5), 105–122.
- El-Heiny, I., and Martini, E. (1981). Miocene foraminiferal and calcareous nannoplankton assemblages from the Gulf of Suez region and correlation. *Géologie Méditerranéenne* 8 (2), 101–108. doi:10.3406/geolm.1981.1159
- El-Heiny, I., and Morsi, S. (1992). Stratigraphic correlation of Neogene sediments in the eastern Nile delta and Gulf of Suez, Egypt. *EGPC, 11th Pet. Expl. Prod.* 1, 166–192.
- El-Naby, A., Abd-Elaziz, W., and Abd-El Aal, M. (2017). Biostratigraphy and seismic data analysis to detect the sequence stratigraphic depositional environment of the Miocene succession: Gulf of Suez (Egypt). *Swiss J. Geosci.* 110, 777–791. doi:10.1007/s00015-017-0277-0
- Fornaciari, E., Backman, J., and Rio, D. (1993). Quantitative distribution patterns of selected lower to middle Miocene calcareous nannofossils from the Ontong Java Plateau. *Proc. ODP. Sci. Results* 130, 245–256. Paper presented at the Berger, WH, Kroenke, LW, Mayer, LA.
- Fornaciari, E., Di Stefano, A., Rio, D., and Negri, A. (1996). Middle Miocene quantitative calcareous nannofossil biostratigraphy in the Mediterranean region. *Micropaleontology* 42, 37–63. doi:10.2307/1485982
- Fornaciari, E., Raffi, I., Rio, D., Villa, G., Backman, J., and Olafsson, G. (1990). “Quantitative distribution patterns of Oligocene and Miocene calcareous nannofossils from the western equatorial Indian Ocean,” in *Proc. ODP, sci. Results*, R. A. Duncan, J. Backman, and L. C. Peterson (College Station, TX: Ocean Drilling Program), 115, 237–254. doi:10.2973/odp.proc.sr.115.153.1991
- Fornaciari, E., and Rio, D. (1996). Latest Oligocene to early middle Miocene quantitative calcareous nannofossil biostratigraphy in the Mediterranean region. *Micropaleontology* 42, 1–36. doi:10.2307/1485981
- Frigola, A., Prange, M., and Schulz, M. (2018). Boundary conditions for the middle Miocene climate transition (MMCT v1. 0). *Geosci. Model Dev.* 11 (4), 1607–1626. doi:10.5194/gmd-11-1607-2018
- Garfunkel, Z., and Batrov, Y. (1977). The tectonics of the Suez rift. *Geol. Surv. Isr. Bull.* 71, 1–44.
- Gartner, S. (1992). Miocene nannofossil chronology in the north atlantic, DSDP site 608. *Mar. Micropaleontol.* 18 (4), 307–331. doi:10.1016/0377-8398(92)90045-1
- Ghorab, M. A., Ebied, Z., and Tewfik, N. (1964). *Oligocene and Miocene rock stratigraphy of the Gulf of Suez area*. Cairo: EGPC Stratigraphic Committee, 1–142.
- Hammer, Ø., and Harper, D. (2006). “Morphometrics,” in *Paleontological data analysis* (Oxford: Blackwell Publishing), 78–156.
- Hammer, Ø., Harper, D. A., and Ryan, P. D. (2001). PAST: paleontological statistics software package for education and data analysis. *Palaeontol. Electron.* 4 (1), 9p.
- Haq, B. U. (1980). Biogeographic history of Miocene calcareous nannoplankton and paleoceanography of the Atlantic Ocean. *Micropaleontology* 26, 414–443. doi:10.2307/1485353
- Hardenbol, J., Thierry, J., Farley, M. B., Jacquin, T., De Graciansky, P.-C., and Vail, P. R. (1998). “Mesozoic and Cenozoic sequence chronostratigraphic framework of European basins,” in *Mesozoic and Cenozoic sequence stratigraphy of European basins 3-13*. Editors C.-P. Graciansky, J. Hardenbol, T. Jacquin, and P. R. Vail (Tulsa: Society for Sedimentary Geology Special Publication), 60.
- Hewaidy, A. G. A., Farouk, S., and Ayyad, H. M. (2013). Foraminifera and sequence stratigraphy of Burdigalian – serravallian successions on the eastern side of the Gulf of Suez, southwestern Sinai, Egypt. *Egypt Neues Jahrb. für*

- Geol. Paläontologie-Abhandlungen 270 (2), 151–170. doi:10.1127/0077-7749/2013/0362
- Hewaidy, A. G. A., Farouk, S., and Ayyad, H. M. (2014). Integrated biostratigraphy of the upper Oligocene–middle Miocene successions in west central Sinai, Egypt. *J. Afr. Earth Sci.* 100, 379–400. doi:10.1016/j.jafrearsci.2014.07.007
- Hewaidy, A. G. A., Mandur, M. M., Farouk, S., and El Agroudy, I. S. (2016). Integrated planktonic stratigraphy and paleoenvironments of the Lower-Middle Miocene successions in the central and southern parts of the Gulf of Suez, Egypt. *Arab. J. Geosci.* 9, 159–232. doi:10.1007/s12517-015-2108-9
- Hume, W. F., Madgwick, T. G., Moon, F. W., and Sadek, H. (1920). Preliminary geological report on Gebel Tanka area. *Pet. Res. Bull.* 4, 1–16.
- Iaccarino, S., Di Stefano, A., Foresi, L., Turco, E., Baldassini, N., Cascella, A., et al. (2011). High-resolution integrated stratigraphy of the upper Burdigalian-lower Langhian in the Mediterranean: the Langhian historical stratotype and new candidate sections for defining its GSSP. *Stratigraphy* 8 (2-3), 199–215. doi:10.29041/strat.08.2.08
- Jamrich, M., Rybár, S., Ruman, A., Kováčová, M., and Hudáčková, N. (2024). Biostratigraphy and paleoecology of the upper Badenian carbonate and siliciclastic nearshore facies in the Vienna Basin (Slovakia). *Facies* 70 (5), 5–31. doi:10.1007/s10347-023-00679-2
- Jovane, L., Florindo, F., Acton, G., Ohneiser, C., Sagnotti, L., Strada, E., et al. (2019). Miocene glacial dynamics recorded by variations in magnetic properties in the ANDRILL-2A drill core. *J. Geophys. Res. Solid Earth* 124 (3), 2297–2312. doi:10.1029/2018jb016865
- Jovane, L., Florindo, F., Wilson, G., de Almeida Pecchiai Saldanha Leone, S., Hassan, M. B., Rodelli, D., et al. (2020). Magnetostratigraphic chronology of a cenozoic sequence from DSDP site 274, ross sea, Antarctica. *Front. Earth Sci.* 8, 563453. doi:10.3389/feart.2020.563453
- Khalifa, M. A., Zaky, A. S., Jovane, L., El-Hewy, A. M., Zahran, E., and Kasem, A. M. (2024). The middle Miocene microfacies, cyclicity, and depositional history: implications on the marmarica Formation at the siwa oasis, western desert (Egypt). *Minerals* 14 (1), 73. doi:10.3390/min14010073
- Krammer, R., Baumann, K.-H., and Henrich, R. (2006). Middle to late Miocene fluctuations in the incipient Benguela Upwelling System revealed by calcareous nannofossil assemblages (ODP Site 1085A). *Palaeogeogr. Palaeoclimatol. Palaeoecol.* 230 (3-4), 319–334. doi:10.1016/j.palaeo.2005.07.022
- Lohmann, G., and Carlson, J. (1981). Oceanographic significance of Pacific late Miocene calcareous nannoplankton. *Mar. Micropaleontol.* 6 (5-6), 553–579. doi:10.1016/0377-8398(81)90021-9
- Lourens, L. J., Hilgen, F., Shackleton, N. J., Laskar, J., and Wilson, D. (2004). “The Neogene period,” in *A geologic time scale 2004*. Editors F. M. Gradstein, J. G. Ogg, and A. G. Smith (Amsterdam: Elsevier), 409–440.
- Maiorano, P., and Monechi, S. (1998). Revised correlations of early and middle Miocene calcareous nannofossil events and magnetostratigraphy from DSDP site 563 (north atlantic ocean). *Mar. Micropaleontol.* 35 (3-4), 235–255. doi:10.1016/s0377-8398(98)00019-x
- Mandur, M. (2009). Calcareous nannoplankton biostratigraphy of the lower and middle Miocene of the Gulf of Suez, Egypt. *Aust. J. Basic Appl. Sci.* 3 (3), 2290–2303.
- Martini, E. (1971). “Standard Tertiary and Quaternary calcareous nannoplankton zonation,” in Proceedings of the Second Planktonic Conference, Roma, China, August 30, 2016. Editor A. Farinacci, 739–785.
- Martini, E., and Worsley, T. (1970). Standard Neogene calcareous nannoplankton zonation. *Nature* 225 (5229), 289–290. doi:10.1038/225289a0
- McGonigal, K. L. (2004). Quantitative Miocene calcareous nannofossil biostratigraphy from the tasmanian gateway. *Geophys. Monogr. Ser.* 151, 191–213. doi:10.1029/151gm12
- McIntyre, A., and Bé, A. W. (1967). Modern coccolithophoridae of the atlantic ocean-I. Placoliths and cyrtoliths. *Pap. Present. A. T. Deep Sea Res. Oceanogr. Abstr.* 14 (5), 561–597. doi:10.1016/0011-7471(67)90065-4
- Monechi, S., Angori, E., and von Salis, K. (2000). Calcareous nannofossil turnover around the Paleocene/Eocene transition at Alamedilla (southern Spain). *Bull. Société géologique Fr.* 171 (4), 477–489. doi:10.2113/171.4.477
- Moustafa, A. R. (1993). Structural characteristics and tectonic evolution of the east-margin blocks of the Suez rift. *Tectonophysics* 223 (3-4), 381–399. doi:10.1016/0040-1951(93)90146-b
- Moustafa, A. R. (2004). “Exploratory notes for the geologic maps of the eastern side of the Suez rift (western Sinai peninsula) Egypt,” in *Geology department* (China: Faculty of Science, Ain Shams University).
- Moustafa, A. R., and Khalil, M. H. (1990). “Structural characteristics and tectonic evolution of north Sinai fold belts,” in *The geology of Egypt*. Editor R. Said (Rotterdam: A.A. Balkema), 381–389.
- NSSC (1974). Rock stratigraphy of Miocene in the Gulf of Suez region. *Egypt. J. Geol.* 18 (1).
- Okada, H. (2000). An improved filtering technique for calculation of calcareous nannofossil accumulation rates. *J. Nannoplankt. Res.* 22 (3), 203–204. doi:10.58998/jnr2188
- Okada, H., and Bukry, D. (1980). Supplementary modification and introduction of code numbers to the low-latitude coccolith biostratigraphic zonation (Bukry, 1973; 1975). *Mar. Micropaleontology* 5 (3), 321–325. doi:10.1016/0377-8398(80)90016-x
- Okada, H., and McIntyre, A. (1979). Seasonal distribution of modern coccolithophores in the western North Atlantic Ocean. *Mar. Biol.* 54, 319–328. doi:10.1007/bf00395438
- Okada, H., and Wells, P. (1997). Late Quaternary nannofossil indicators of climate change in two deep-sea cores associated with the Leeuwin Current off Western Australia. *Palaeogeogr. Palaeoclimatol. Palaeoecol.* 131 (3-4), 413–432. doi:10.1016/s0031-0182(97)00014-x
- Patton, T. L., Moustafa, A. R., Nelson, R. A., and Abdine, A. S. (1994). “Tectonic evolution and structural setting of the Suez rift,” in *Interior rift basins*. Editor S. M. Landon (Memoir: American Association of Petroleum Geologists), 59, 9–55. doi:10.1306/m59582c2
- Pea, L., Bohaty, S. M., and Villa, G. (2011). Calcareous nannofossil fragmentation as a dissolution proxy: a case study from the eocene-oligocene transition at odp site 1090 (agulhas ridge, south atlantic ocean). *Berichte Geol. Bundesanst.* – 85, 127.
- Perch-Nielsen, K. (1985). “Cenozoic calcareous nannofossils,” in *Plankton. Stratigraphy*. Editors H. M. Bolli, J. B. Saunders, and K. Perch-Nielsen (USA: Cambridge Earth Science Series), 427–554.
- Persico, D., and Villa, G. (2004). Eocene–oligocene calcareous nannofossils from maud rise and kerguelen plateau (Antarctica): paleoecological and paleoceanographic implications. *Mar. Micropaleontol.* 52 (1-4), 153–179. doi:10.1016/j.marmicro.2004.05.002
- Plaziat, J.-C., Montenat, C., Barrier, P., Janin, M.-C., Orszag-Sperber, F., and Philobos, E. (1998). “Stratigraphy of the Egyptian syn-rift deposits: correlation between axial and peripheral sequences of the north-western Red Sea and Gulf of Suez and their relations with tectonics and eustasy,” in *Sedimentation and tectonics in rift basins: red sea–gulf of aden*. Editors B. H. Purser, and D. W. J. Bosence (London: Chapman & Hall), 77–96.
- Raffi, I., Agnini, C., Backman, J., Catanzariti, R., and Pälke, H. (2016). A Cenozoic calcareous nannofossil biozonation from low and middle latitudes: a synthesis. *J. Nannoplankt. Res.* 36, 121–132. doi:10.58998/jnr2206
- Raffi, I., Backman, J., Fornaciari, E., Pälke, H., Rio, D., Lourens, L., et al. (2006). A review of calcareous nannofossil astrobiochronology encompassing the past 25 million years. *Quat. Sci. Rev.* 25 (23-24), 3113–3137. doi:10.1016/j.quascirev.2006.07.007
- Raffi, I., and Flores, J.-A. (1995). “Pleistocene through Miocene calcareous nannofossils from eastern equatorial Pacific Ocean,” in *Proceedings of the ocean drilling program, scientific results*. Editors N. G. Pisias, L. A. Mayer, T. R. Janecsek, A. Palmer-Julson, and T. H. van Andel (College Station, TX: Ocean Drilling Program), 138, 233–286.
- Rio, D., Fornaciari, E., and Raffi, I. (1990). Late Oligocene through early Pleistocene calcareous nannofossils from western equatorial Indian Ocean (Leg 115). *Proc. ODP. Sci. Results* 115, 175–235. Paper presented at the Duncan, R. A., Backman, J., Peterson, L. C.
- Sellwood, B., and Netherwood, R. (1984). Facies evolution in the Gulf of Suez area: sedimentation history as an indicator of rift initiation and development. *Mod. Geol.* 9, 43–69.
- Shahin, A., and El Baz, S. M. (2021). Biostratigraphy and paleobiogeography of the Early-Middle Miocene ostracods and foraminifera from the northern part of the Gulf of Suez, Egypt. *J. Afr. Earth Sci.* 182, 104252–252. doi:10.1016/j.jafrearsci.2021.104252
- Shevenell, A. E., Kennett, J. P., and Lea, D. W. (2004). Middle Miocene Southern Ocean cooling and antarctic cryosphere expansion. *Science* 305, 1766–1770. doi:10.1126/science.1100061
- Shevenell, A. E., Kennett, J. P., and Lea, D. W. (2008). Middle Miocene ice sheet dynamics, deep-sea temperatures, and carbon cycling: a Southern Ocean perspective. *Geochem. Geophys. Geosystems* 9 (2). doi:10.1029/2007gc001736
- Takahashi, K., and Okada, H. (2000). The paleoceanography for the last 30,000 years in the southeastern Indian Ocean by means of calcareous nannofossils. *Mar. Micropaleontol.* 40 (1-2), 83–103. doi:10.1016/s0377-8398(00)00033-5
- Theodoridis, S. (1984). Calcareous nannofossil biozonation of the Miocene and revision of the helicoliths and discoasters. *Utrecht Micropaleontol. Bull.* 32, 272p.
- Turco, E., Cascella, A., Gennari, R., Hilgen, F. J., Iaccarino, S. M., and Sagnotti, L. (2011). Integrated stratigraphy of the La vedova section (conero riviera, Italy)

and implications for the burdigalian/langhian boundary. *Stratigraphy* 8 (2), 89–110. . doi:10.29041/strat.08.2.02

Villa, G., and Persico, D. (2006). Late Oligocene climatic changes: evidence from calcareous nannofossils at kerguelen plateau site 748 (southern ocean). *Palaeogeogr. Palaeoclimatol. Palaeoecol.* 231 (1-2), 110–119. . doi:10.1016/j.palaeo.2005.07.028

Wade, B. S., and Bown, P. R. (2006). Calcareous nannofossils in extreme environments: the Messinian salinity crisis, Polemi Basin, Cyprus. *Palaeogeogr. Palaeoclimatol. Palaeoecol.* 233 (3-4), 271–286. doi:10.1016/j.palaeo.2005.10.007

Wei, W., and Wise, S. W. (1990). Biogeographic gradients of middle eocene-oligocene calcareous nannoplankton in the south atlantic ocean. *Palaeogeogr. Palaeoclimatol. Palaeoecol.* 79 (1-2), 29–61. doi:10.1016/0031-0182(90)90104-f

Wei, W., and Wise, S. W. (1992). Eocene-Oligocene calcareous nannofossil magnetobiochronology of the Southern Ocean. *Newsletters Stratigr.* 26, 119–132. doi:10.1127/nos/26/1992/119

Ziveri, P., Thunell, R., and Rio, D. (1995). Seasonal changes in coccolithophore densities in the Southern California Bight during 1991–1992. *Deep Sea Res. Part I Oceanogr. Res. Pap.* 42 (11-12), 1881–1903. doi:10.1016/0967-0637(95)00089-5